FLOOD RISK ASSESSMENT FOR (120MWp) SOLAR PV POWER PROJECT KARACHI

AT

DEH HALKANI DISTRICT WEST, KARACHI SINDH PAKISTAN

FINAL REPORT

Directorate of Alternate Energy,
Energy Department, Government of Sindh (DAE GOS)

Renewable Resources (Pvt) Ltd (RE2)
1002, 10th Floor, Green Tower Jinnah Avenue, Blue Area,
Islamabad, Pakistan
https://www.renewableresources.com.pk/

Review and Approval Sheet

TITLE : Flood Risk Assessment for (120MWp) Solar PV Power Project at Karachi site 03 – Deh Halkani District West, Karachi Sindh Pakistan

DOCUMENT NUMBER : RE2-321-231-002-Rev 01

CLASSIFICATION : CONTROLLED

SYNOPSIS:

This document is a Flood Risk Assessment for (120MWp) Solar PV Power Project at Karachi Site 03 – Deh Halkani, District West, Karachi Sindh Pakistan.

PREPARED BY :

Saif Ullah
Environment & GIS Expert
saif@renewableresources.com.pk

REVIEWED BY :

Junaid Safdar
General Manager Technical
junaid@renewableresources.com.pk

APPROVED BY :

Ammad Riaz
Chief Technical Officer (CTO)
info@renewableresources.com.pk

Date : 10th September, 2024

Document Restriction Level

Restricted Document √ Unrestricted Document ×

Table of Contents

List of Figures

List of Tables

List of Annexures

Abbreviations and Acronyms

AMSL	Above Mean Sea Level
ASL	Above sea level
CFS	Cubic feet per second
DC	Data Coverage
DEM	Digital Elevation Model
DMS	Degree minute second
ECMWF	European Centre for Medium-Range Weather Forecasts
ERDAS	Earth Resources Data Analysis System.
FAO	Food and agriculture organization
GIS	Geographic information system
HEC-GeoRAS	Hydrological Engineering Centre – Geospatial River Analysis System
HEC-RAS	Hydrologic Engineering Center - River Analysis System
IEC	International Electrotechnical Commission
LOI	Letter of Intent
LULC	Landuse and Landcover
MERRA	The Modern Era Retrospective analysis for Research and Applications
MWh	Mega Watt hours
MWh	Mega Watt
NASA	National Aeronautics and Space Administration
PO	Probability of exceedance
RP	Return period
SCS	Soil Conservation Service
SRTM	Shuttle Radar Topography Mission
TC	Time concentration
TIN	Triangular Irregular Network
UTM	Universal Transverse Mercator
WGS84	World Geodetic System 1984

Contact Information's

PROJECT CONSULTANT:

RENEWABLE RESOURCES (Pvt.) LTD (RE2)	
Islamabad Office	1002, 10th Floor, Green Towers, Jinnah Avenue, Blue Area, Islamabad, Pakistan Tel: 0092 51 8358591 Fax: 0092 51 8358592
Website	www.renewableresources.com.pk
Contact Person	Junaid Safdar General Manager Technical
Email	junaid@renewableresources.com.pk

PROJECT SPONSORS (CLIENT):

Sindh Solar Energy Project, Energy Department, Government of Sindh (DAE GOS)	
Address	Banglow F3, Forum Street, Near the Forum, Clifton Block 9, Karachi
Website	www.sindhenergy.gov.pk
Contact Person	Mehfooz Qazi
Designation	Project Director
Email	pd.uss@ssep.gos.pk

1 EXECUTIVE SUMMARY

The Flood Risk Assessment report for the Deh Halkani PV Solar Site were prepared for the Energy Department of the Government of Sindh (DAE GOS) to assess the potential sources of flooding that may impact the project site and to determine the impact of the proposed development on flooding and flood risk to surrounding lands and properties. The Halkani PV Solar facility located within the designated solar park in Gadap Town, West Karachi, Sindh. The study analyzed various data points, including meteorological data (precipitation and temperature) from the period of (1999 - 2022), as well as topography, terrain, land use and cover, geological conditions and surroundings, and other relevant parameters. The project site encompasses an area of approximately 612 acres and is situated at coordinates 66°59'35.97"E longitude and 25° 1'22.34"N latitude.

The report utilized advanced software such as ArcGIS, HEC-RAS, and HEC-GeoRAS to analyze catchment characteristics, including runoff and natural stream networks, and analyzed rainfall data obtained from nearby gauge stations, satellite-based TRMM, and SolarGIS to evaluate flood conditions at the site and surrounding areas. Flood inundation maps were generated through ArcGIS and HEC-RAS modeling, indicating the extent of flooding under different scenarios. The report also incorporated a hydrology analysis to determine flood peak hydrographs and performed a frequency analysis to quantify the magnitude of extreme storm events for specified return periods.

Following simulations and the identification of flood inundation in the project land and its susceptibility, a flood analysis was carried out based on the meteorological data and a digital elevation model (DEM) of the project site. The analysis was performed while considering the observed flood range and calculated discharges. The minimum and maximum elevations of the land were determined from the topographic survey map of the project area.

The project site's topography is characterized by disturbed elevations. While the southeast portion of the site is narrow and has small hills, the terrain of the project land is not uniform. The northwest section also features moderate to steep slopes to some extent, with a peak elevation of 83 meters. A large, flat section of the land generally lies at elevations below 46 meters. The upper reaches of the project area are less likely to be impacted by flood inundation. However, the lower reaches of the area, which are characterized by low slopes and uneven terrain, are more susceptible to flood inundation during heavy rainy seasons and flash floods. Therefore, it may be necessary to implement civil infrastructure measures to prevent water stagnation in certain areas. According to the analysis results, the overall flood risk to the project is considered low. The report concludes with an assessment of potential flood risk and recommendations for future actions.

2 INTRODUCTION

This report has been compiled to conduct a flood risk assessment and evaluation study for the "PV Solar Project Deh Halkani, West Karachi Sindh, Pakistan." The study incorporates primary datasets gathered from field surveys and secondary datasets from desktop research. The flood risk assessment and evaluation study were conducted at the Halkani project site during field surveys.

The topography of the project site suggests a minor to moderate elevation towards the southeast and southwest, with a substantial flat expanse in the mid-center towards the north. The middle portion of the project plot has small, steep hills with elevations ranging from 53 to 83 meters. Generally, the elevation at the site remains below 83 meters above sea level. The land within the site is mostly barren, lacking any form of vegetation, with only a few patches of agricultural land. Furthermore, there are few public rights of way that traverse the area.

3 GENERAL DESCRIPTION

As part of the project, both desktop studies and field surveys were conducted. Desktop studies involved collecting climate and hydrological data, as well as published information on the environmental characteristics of the plot area, such as topography, vegetation, soil, lithology, land use, and land cover. Field surveys, on the other hand, consisted of a field assessment, topographic survey, geotechnical investigations, and mapping of the area, water bodies, critical infrastructure, risk scoring analysis, and other studies to facilitate the construction of a PV solar park infrastructure.

3.1 Location of the project site

The project is located at 66°59'28.66"E longitude and 25°1'57.48"N latitude, covering a land area of approximately 612 acres within the jurisdiction of the Malir district, Sindh province, Pakistan, as shown in (**Figure 3-1**). The site is situated approximately 30-40 km from Karachi city, and the elevation of the Halkani site ranges from 37 m to 83 m above sea level.

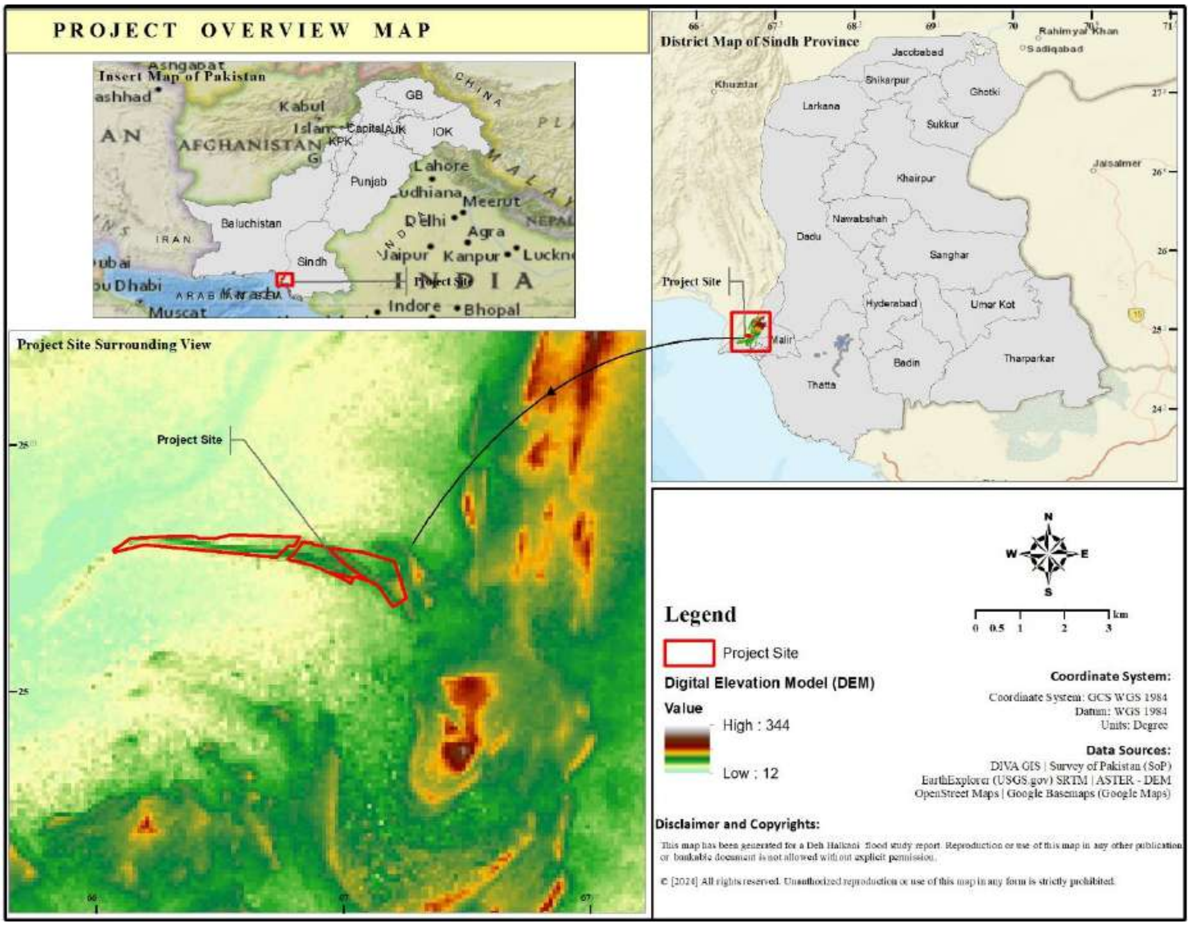

Figure 3-1: Site Location overview map

3.2 Project Site Description

The project site is located off Karachi Northern Bypass in Deh Halkani, Gadap Town West Karachi, Sindh, Pakistan, along the M-10 motorway. The topography of the area is not flat, with notable elevation changes observed across the site. The majority of the site is barren, with bushes and small patches of agricultural land. In some locations, temporary settlements exist.

The climate of the project area is characterized by fluctuating temperatures and sparse rainfall. The summers are hot and humid, with average temperatures ranging between 30°C to 34°C. The topography of the project site is such that the land is slightly elevated to the southeast and northwest, with a large flat section generally at elevations below 83 m. Some pictures from the site are attached below for better understanding.

Data collecting includes: i) meteorological data from both gauged nearby stations as well satellite-based or re-analysis models, ii) satellite data SolarGIS, iii) published materials/maps/reports etc. Data processing contains multistage processes of obtained data to use in flood inundation modelling and rainfall-runoff modelling requires several comprehensive data layers from the targeted study area.

According to the project tasks, flood risk assessment studies, field surveys, mapping, and evaluations undertaken in the plot area were based on a series of approaches and methods such as data collection, data processing, and validation, hydrological modeling, flood inundation mapping, and visualization in a GIS environment, field assessment, and mapping. HEC-RAS, HEC-GeoRAS, ArcGIS, and ERDAS Imagine software were used for modeling and mapping. A detailed description of the methods and approaches applied is presented in the corresponding sections.

Figure 3-2: Project Site View

4 SCOPE OF WORK

This report presents a comprehensive evaluation of the flood risk in the project area, including a detailed analysis of the project's topography and the surrounding topographic features. The geographical characteristics of the area were analyzed through a comprehensive hydrological study of the sub-region, aimed at gaining a thorough understanding of the behavior of sub-basins, streams, rainfall, and tributaries.

The scope of work covered within this study includes:

- An examination of all potential sources of flooding that may impact the project site
- An evaluation of the potential impact of flooding on the site, including the consideration of flood zones and demonstration that the development meets the vulnerability criteria outlined in the guidance.
- Characterization of catchment features, such as runoff and natural stream networks, using leading software like ArcGIS, HEC RAS, and HEC - GeoRAS. These features are further analyzed for flood analysis and appropriate drainage design.
- Analysis of the potential impact of the proposed development on flooding and flood risk to adjacent lands and properties.
- Analysis of rainfall data obtained from nearby gauge stations or satellite-based TRMM data to determine flood conditions at the site and surrounding areas.
- Identification of any structures that may impact the hydrology and analysis of hydrology to derive flood peak hydrographs and frequency analysis to determine the magnitude of extreme storm events for specified return periods.
- Creation of a Flood Inundation map showing flood zones on the subject site/area, considering the advancements in remote sensing techniques, including the strength and limitations of MODIS, Landsat, Sentinel, and other satellite data, as well as drone imagery.
- Based on parameters such as rainfall intensity, runoff, catchment area, runoff coefficient, existing soil conditions, drain outfall location, etc. derived from the hydrology study, the plant layout and designs for stormwater drains and culverts are planned.
- The study includes an analysis of both Pre and Post-development conditions.
- A conclusion of the study outlining the potential flood risk and future recommendations.

5 ENVIRONMENTAL CHARACTERISTICS OF THE PROJECT SITE

5.1 Geology of the Area

The deposition of the area mainly consists of ‘dense to very dense, gravel’, ‘medium dense to very dense, sand’, ‘very stiff to hard, silt’ and ‘very stiff, clay’. Groundwater table was not encountered up to the explored depth of 5.0 meters in any of the boreholes drilled at the site, during this investigation. The deposition of the area mainly consists of ‘medium dense to very dense, fine to coarse grained, silty, sand, very stiff to hard, sandy, clayey, silt, very stiff to hard, sandy, silty, clay and distinctly weathered, sandstone. Groundwater table was not encountered up to the explored depth of 5.0 meters in any of the boreholes drilled at the site, during geotechnical investigations. This area lies in the east of Kirthar ranges. Geologically this area contains the exposed Cenozoic rocks from Paleocene to Recent Deposits. The exposed formation of Eocene age is Laki formation. Nari formation of Oligocene age, Gaj formation of Miocene and Machair Formation of Miocene-Pliocene ages are exposed at various localities in the district. The surface is covered by recent cover of unconsolidated surficial deposits of silt, sand and gravel.

5.2 Seismicity of the Area

The project site is located in Zone 2B as per “Seismic Provisions-2007” of Building Code of Pakistan. This zone indicates moderate degree of damage during the seismic loading. Keeping in view the seism tectonic set up of the project site and the degree of importance of the structures of the proposed project, it is recommended that the structures should be designed to withstand maximum horizontal peak ground acceleration (PGA) of 0.06 – 0.16g. This PGA has 10% probability of exceedance in 50 years.

As per Building Code of Pakistan (BCP), Seismic Provisions-2007 following earthquake data can be considered for the project site:

- Seismic Zone, as per table 2.2 of BCP - 2007: 2B
- Seismic soil profile has been taken as ‘SD’ for the foundations in accordance with UBC-97 based on SPT N method approach.

5.3 Climatic conditions

According to the project tasks, the climate of the plot area Deh Halkani site is required to be analyzed from two aspects: (i) general climate characteristics of the project area and (ii) rainfall analysis in view of hydrological modelling. For this purpose, this section will briefly describe climate characteristics of the plot area based on data collected from nearest weather stations. Due to the lack of weather stations, precise data on the climate of the plot area is not available therefore the satellite verified data are collected from (SolarGIS [1] and Power Larc Nasa gov [2]).

The typically climate of the Project area can be broadly classified as arid, moderate, hot and humid. The mild winter is restricted to the December-February period. The summer extends from March to November, which overlaps the short spells of the main rainy season during July-August. The weather tends to be very humid during June, July, August and September and is pleasant during February and March.

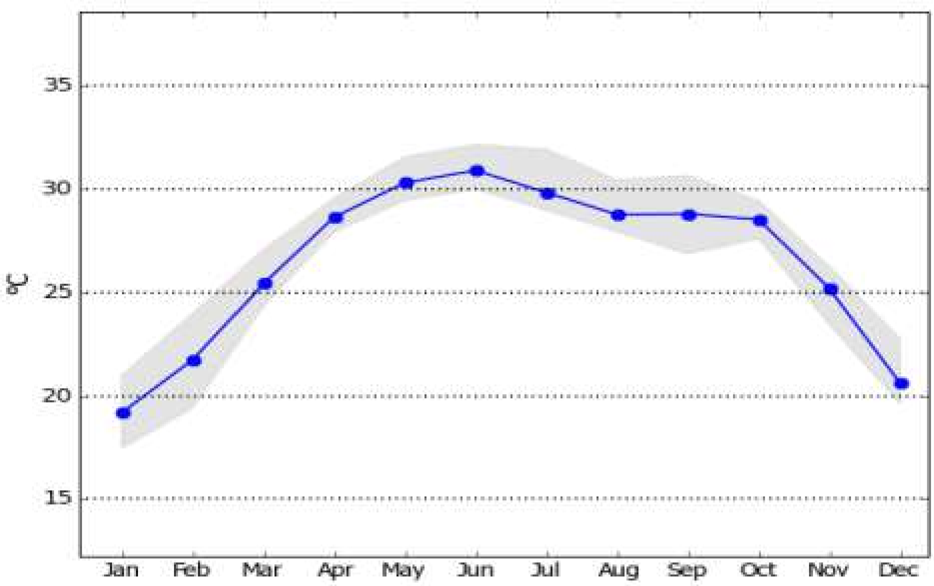

Figure 5-1: Monthly long-term average, minimum and maximum [°C] profile

The climate of this area is characterized by fluctuating temperatures and sparse rainfall. The summer seasons are hot and humid with average temperatures ranging between 30°C to 35°C. The temperature in summer seasons may reach up to 45°C. The winters are pleasant with average temperature in the range of 15°C to 20°C. The months of July and August generally observe the annual monsoon rainfalls. The climate information of the project site is shown in (

Table 6-2), (**Figure 5-3**: Interannual variability of yearly values precipitation .

---

[1] Solar GIS Data

[2] Spatially disaggregated from CFSv2 and GFS (© 2022 NOAA) and ERA5 (© 2022 ECMWF) by Solargis method

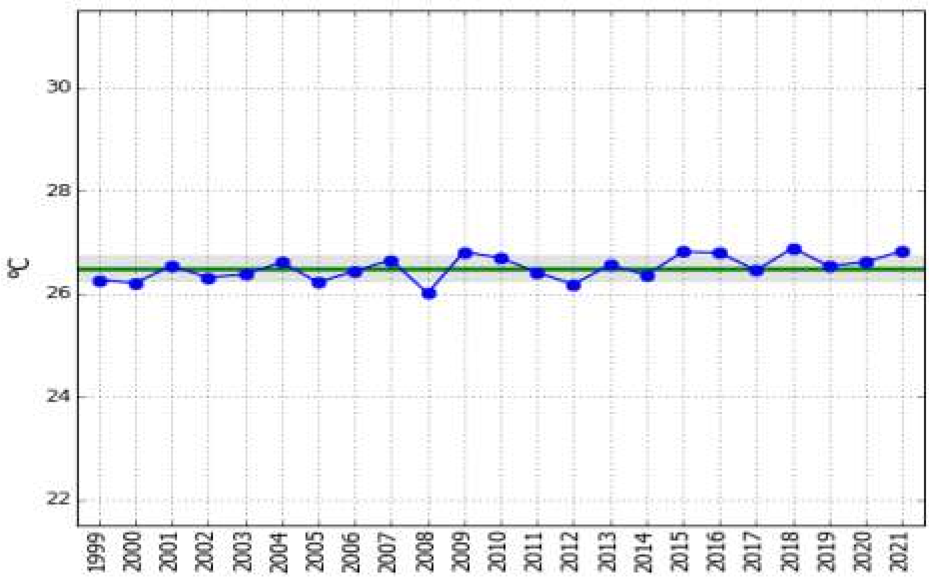

Figure 5-2: Interannual variability of yearly values with average line and STDEV band

The inter-annual variability of the yearly sum of precipitation values over the long-term is depicted in the accompanying (**Figure 5-3**: Interannual variability of yearly values precipitation long-term. It can be observed that precipitation has increased over a 5-year span, with the peak precipitation occurring in the year 2022.

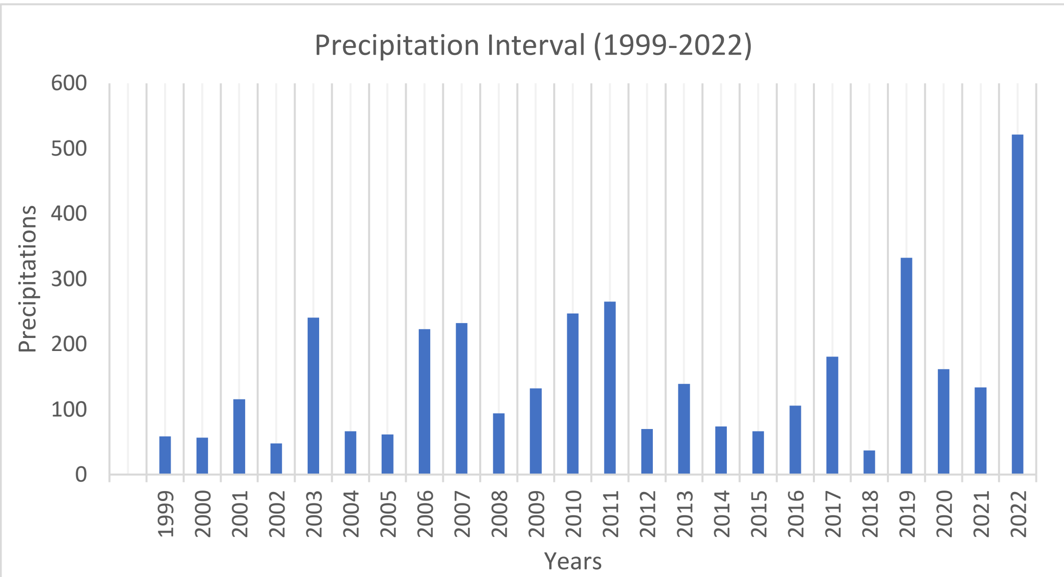

Figure 5-3: Interannual variability of yearly values precipitation long-term

The average monthly temperature of the project site, as well as the sum of precipitation, are presented in the accompanying (**Figure 5-4).** The analysis of meteorological data is further detailed in (Section 6) of this report.

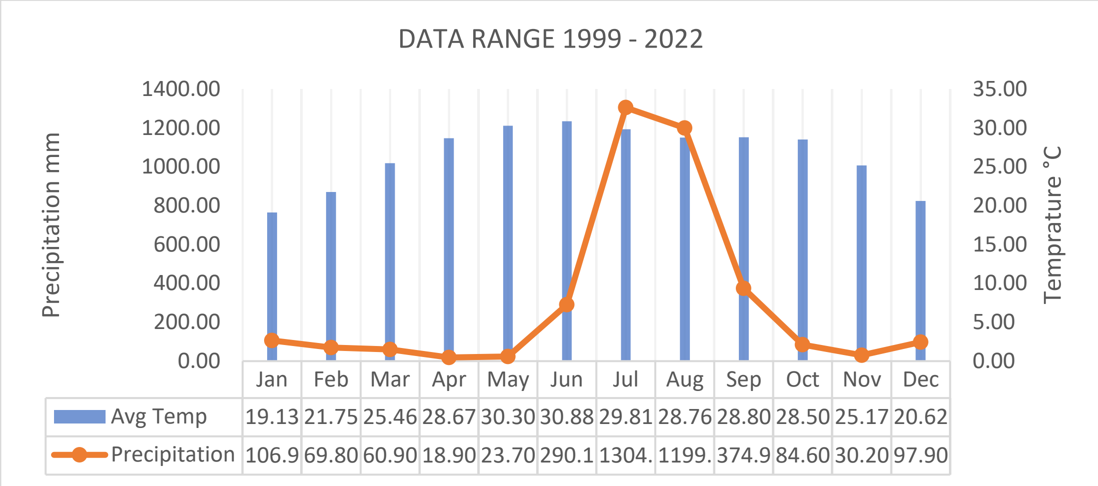

Figure 5-4: Average monthly temperature variation [°C] and precipitations (mm) profile

5.4 Hydrology

The hydrographic network is developed in the Deh Halkani plot site, terrain of the site is sub-arid and dry steppe climate with hot and dry summers and mild winters. It is located at an elevation of 153 meters above sea level. The project area primarily serves as a watershed for several small basins (**Figure 6-1**). One of them and the western part with a large area belongs to the HUB river basin. Other local small area of basins is characterized by seasonal flow, and they belong directly to the HUB river and Arabian sea. The valleys in the region are known as dry valleys because of their local basin area in combination with arid environment. A major part of the plot area belongs to the basin of the river called HUB river. This basin covers the entire northern part of the plot site with seasonal stream flowing southward into the Arabian Sea. The slopes of the HUB river valley are surrounded by small hills sharply divided by gully. Although the river has very small and temporary flows, it has a small riverbed **(Figure 5-5).** This factor indicates that floods occur during the rainy season, which expands the river basin. It has been planned that, solar installations are to be placed in the watershed of HUB river and other perennial tributaries. PV solar installations have been destined at an average altitude of 2 km from the main riverbed. The difference in height between the riverbed and the PV site is at least 103 m. Majority of the project area, north of the central watershed, covers several local basins. Unlike the HUB river valley, the slopes of the valleys in this part of the plot site are not sharply fragmented by gullies. This is due to the relatively gentle slope of the area and aspect. In these valleys, temporary streams are formed in spring and autumn owing to the small drainage area. Therefore, these catchments prone potentially no severe floods. The eastern mountainous part of the plot area encompasses the basin of the rain water ways, which has the second largest watershed after the HUB river. The streams of this watershed are towards southerly direction and there is no strong fragmentation with river valleys and gullies. The distance between the designed PV solar locations and mainstream of the local basins is significantly long.

The catchments present in the plot site and hydrographic network within the plot area was generated using DEM with 12.5m spatial resolution. (**Figure 5-5)** presents hydrographic network of seasonally formed streams in the area. In the central part of the plot area, there is a natural salty lake at an altitude of 70m above sea level.

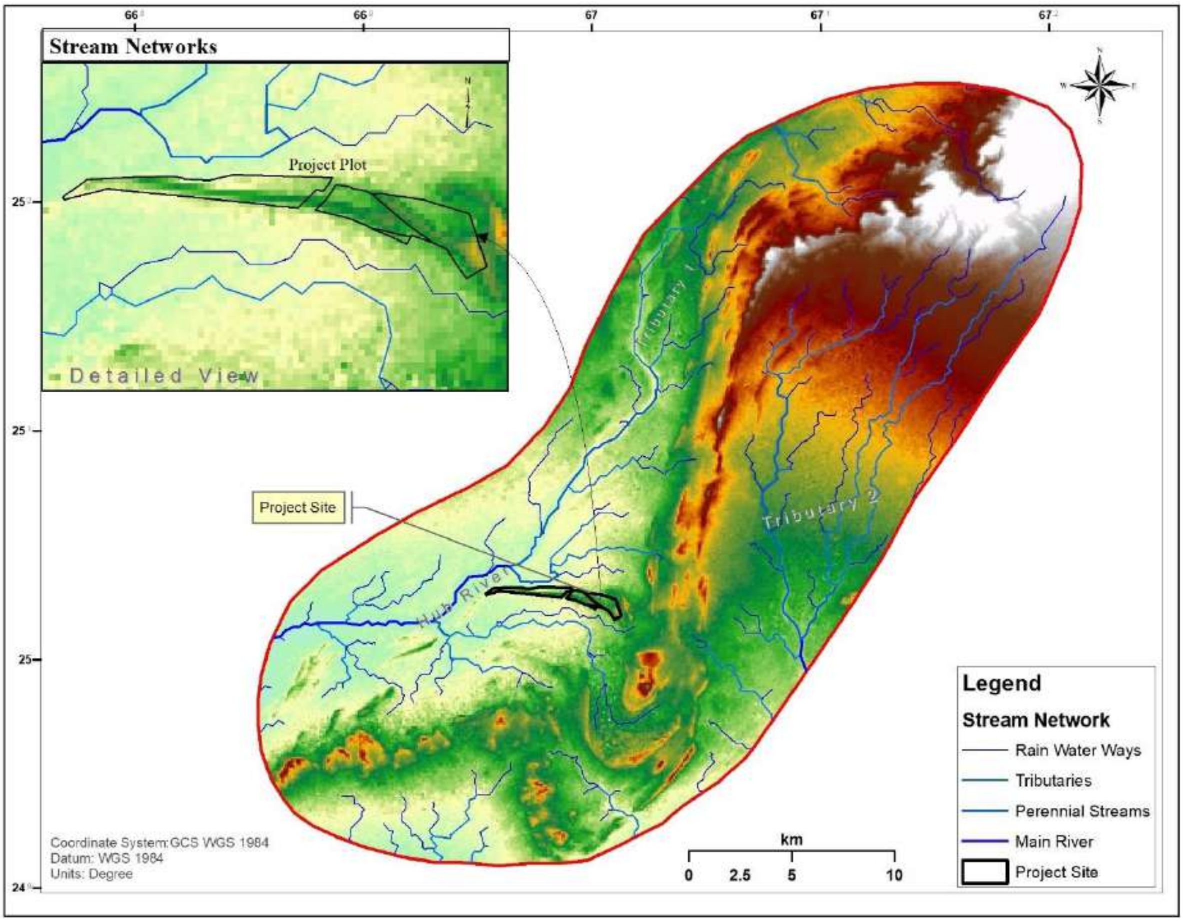

Figure 5-5: Hydrographic set of the local catchments in the Deh Halkani plot site.

Figure 5-6: Riverbed of the HUB River in the east part of the plot site

5.5 Flood Sources

The province of Sindh experiences two types of flooding: riverine and torrential. Riverine floods are more predictable and provide ample time for response, whereas torrential floods offer little warning and have a higher intensity. These floods typically occur during the monsoon months of July and August, when heavy rains occur in the catchment areas in Balochistan. The western boundary of Sindh is connected to Baluchistan through the Kirthar hills.

In 2011, a series of torrential floods resulted in significant devastation across Kacha and the surrounding areas of Sindh. Over 11,000 villages were impacted, displacing more than 213,000 households and resulting in the loss of over 1,065,000 livestock. District Larkana, one of the oldest districts in Sindh, was particularly affected by the floods. The floods were caused by the overflow of the River Indus and its tributaries, which often results in flooding in the northern and southern regions of Sindh province. The upper region of Sindh province, comprising the districts of Jacobabad, Shikarpur, Larkana, Kashmore, Qambar, Shahdadkot, Jamshoro and Dadu on the left bank of the River Indus and Ghotki, Sukkur, Khairpur, Naushahro Feroze and Matiari on the right bank of the River Indus, are particularly susceptible to severe flooding when the River Indus is in high flood. The districts in lower Sindh that are prone to riverine flooding include Dadu, Jamshoro and Thatta on the left bank of the River Indus and Tando Muhammad Khan, Hyderabad on the right bank. According to the flood map of Pakistan, Sindh province is considered to be in a moderate to heavy flooding zone shown in **(Figure 5-7) .**

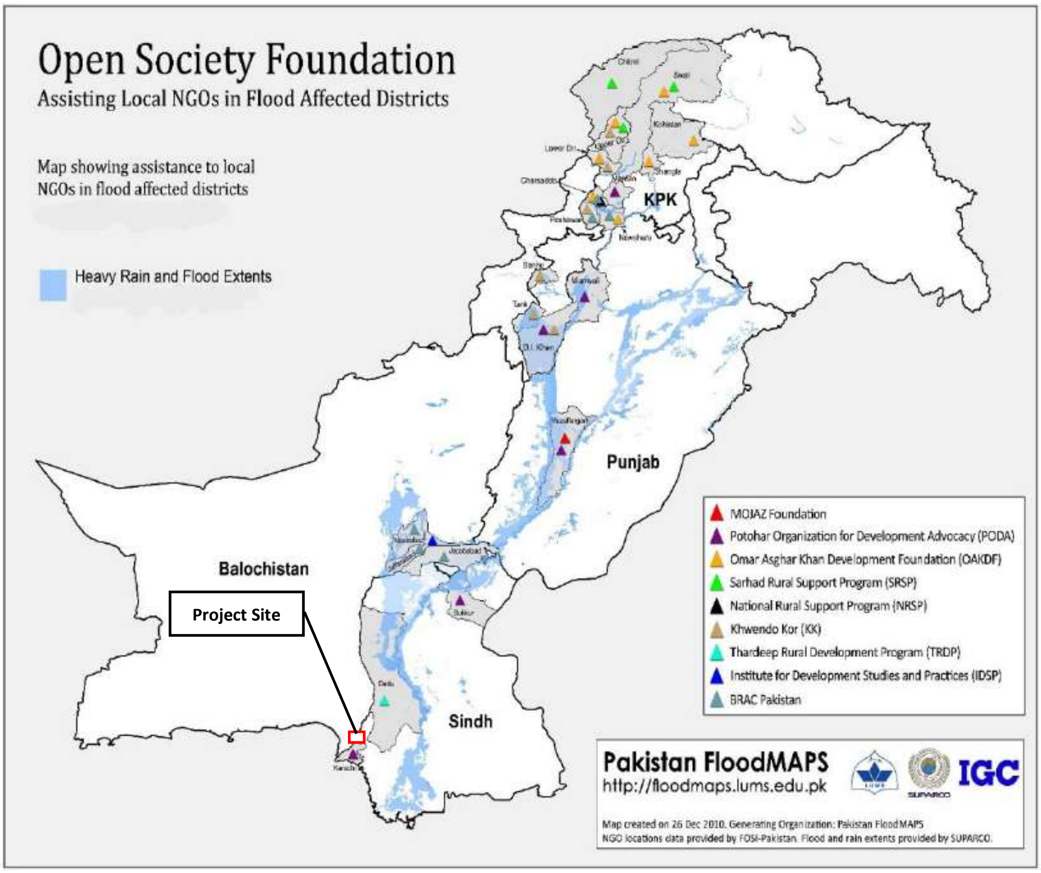

Figure 5-7: Flood Map of Pakistan

5.6 Topography

The area of the plot site is hypsometrically diverse ranging its elevation from the Arabian Sea level to 83 m. The general view of the relief of this region is determined by intermontane depression of foothill and hillslopes, hill ridge, planation surface, marine terrace and plains. These landforms were formed under the predominance of exogenous factors along with endogenous factors. The substantial role of arid-denudation, erosion-denudation, abrasion and accumulation processes in the formation of the relief is clearly depicted. From the geomorphological point of view, this region is considered as a folded morpho structure and the characteristic structures include anticlinal and monoclinal ridges, syncline valleys and plateaus. Regarding its topographical conditions and relief forms, the area of plot site is considered a special region.

The slopes of the plot area generally gentle and dominantly north and south faced. The hill slopes in particular south-faced slopes have undergone both sheet and gully erosion. The spread of erosion processes in these places is not only limited to water erosion, but also deflation contributes significantly. Consequently, the topsoil or the soil profile at large has been subjected to an utter wash-off enabling the clay rocks to appear on the surface. The elevation of the watershed line increases from east to west and slopes are generally gentle. According to the FAO Soil Classification System (WRB-World Reference Base for Soil Resources 2016) accommodating soil type include Loamy.

5.7 Photographical Documentation

Site consists of flat terrain from South to east direction. Most of land is generally barren with small agriculture around. East North side of the plot site has HUB river flowing from north to south direction. River is seasonal with high level expected during summer season from (June - August) and low level expected during Winters (November - March). The 360° view of the site is shown in below **(Figure 5-8), (Figure 5-9).**

Figure 5-8: Deh Halkani (West – North View)

Figure 5-9: Deh Halkani (South - East View)

6 DESCRIPTION AND SOURCES OF THE DATA

The flood risk assessments were carried out as part of the study's objectives using the following data sets and tools:

- Collection of topographic data
- Collection of meteorological data, including temperature and rainfall
- Generation of a Digital Elevation Model (SRTM - 30 meters)
- Delineation of watersheds and identification of stream networks
- Collection of flow data, including stream discharge
- Analysis of land use and land cover data
- Soil data
- Analysis of precipitation data from 1999-2022 for maximum daily precipitation and annual precipitation trends
- Utilization of software such as HEC-RAS, ArcGIS, and HEC-GeoRAS extension for 3D modeling
- Simulation of flood conditions models.

6.1 Hydrology Data

The Halkani plot site belongs to the HUB-River hydrological region according to its physical and geographical conditions. Hydrographic river set in the plot area and adjacent places is characterized by small seasonal streams. The designed plot area is in the watershed of small catchments (**Figure 6-1).** Therefore, no gauging station and hydrometric records are originally available from their discharges. However, published materials, books, articles, hard copy maps e.g., regarding hydrologic and hydrographic characteristics of the plot area were collected.

A low drainage density with approximately 4360.22 (cfs) is typical to this region. The main flow occurs during single seasons, June-August and even cause seasonal floods. The high relative humidity in this season and the presence of sparse vegetation, ravines and balkas in the area cause short-term floods. The water volume of these rivers varies in the range of 1474.84 (cfs) – 15816 (cfs)

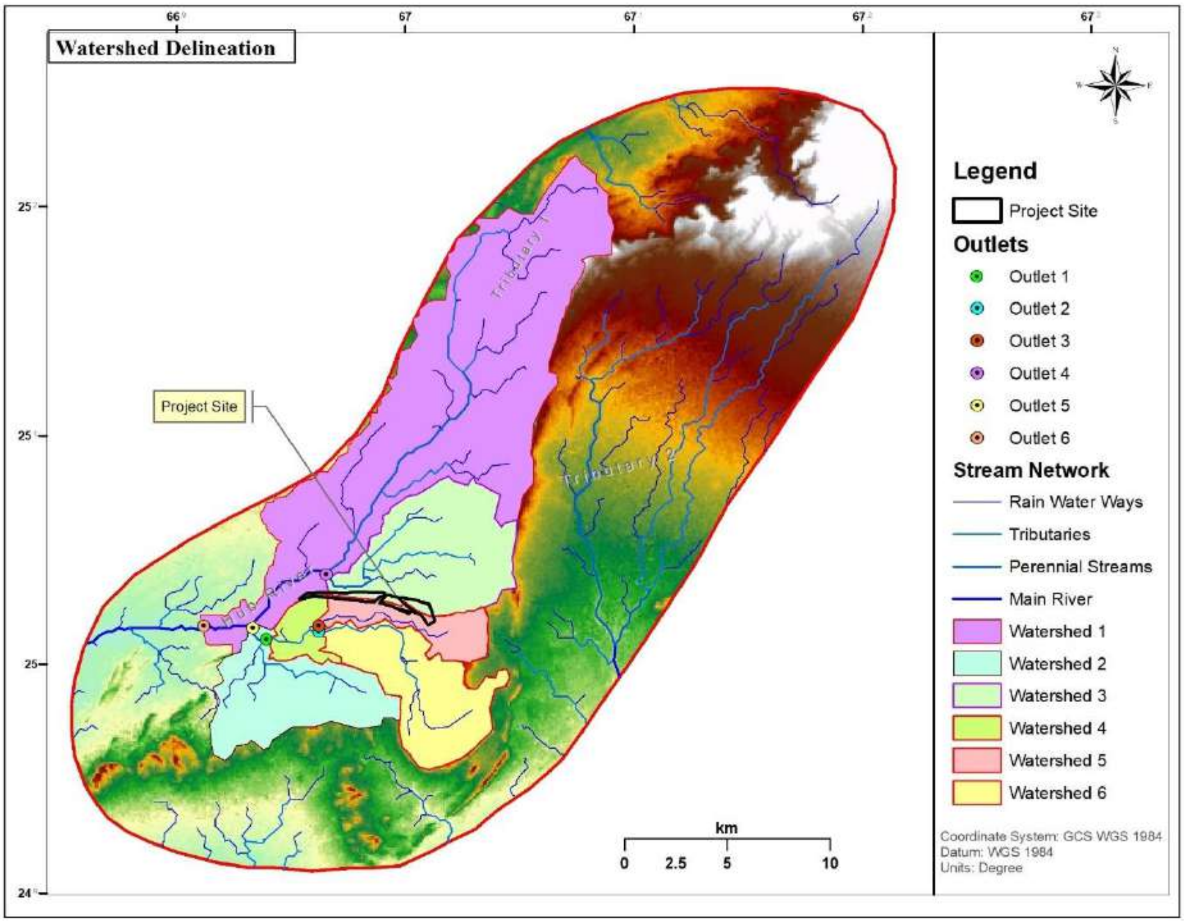

Figure 6-1: Watershed delineation of Deh Halkani site and adjacent.

The primary challenge faced by this study is the shortage of data regarding stream discharges in the study area. To address this issue, an initial estimation was conducted to calculate flow and flood patterns in the catchments. In addition, daily discharges of the local streams in the plot area were simulated using traditional methods, which will be described in subsequent sections of the report. The plot area includes six catchments, with the basins of these streams partially or fully within the plot area. The largest of these catchments, covering the north part of the plot site, is the HUB river. It originates from the northern slope of the peaks at an altitude of 1059m at the northeastern end of the uphill range. The HUB dam located in the upper reach of the project plot catchment area, and the river flows throughout the year, eventually reaching the Arabian Sea.

Rainwater comprises a major portion, 90-95%, of the stream, unlike underground waters. The HUB river has a length of 56 km and a basin area of 134 km. The average width of the basin is 2.4 km and the average height is 520 m. Small shrubs can be found in the river basin.

The Rational Method is commonly used to determine the discharges of storm sewers, channels, and other drainage structures. The stream discharges of the river and tributaries in the plot site were estimated using the following formulas:

$$Q_p = CiA$$

$$i = \frac{precipitation\left(\frac{mm}{annum}\right)}{Time(annual)}$$

$$V = A \times i$$

where

Q_p= Peak Discharge (cubic feet/sec)

C=Runoff coefficient

i= Intensity (inch/hour)

V= Volume (cubic feet/sec)

A= Area (acres)

The Rainfall intensity $'i'$ is typically found from Intensity/Duration/Frequency curves for rainfall events in the geographical region of interest. The duration is usually equivalent to the time of concentration of the drainage area. The storm frequency is typically stated by local authorities depending on the impact of the development. A 10-yr, 25-yr, 50-yr, or even 100-yr storm frequency may be specified.

The annual flow rate in the Halkani plot area is depicted in the(**Figure 6-3)**. The data, which spans from (1999 – 2022), shows that the minimum flow of the stream occurs between September to April, while the peak flow occurs between June to August. The flow rate is measured in cubic feet per second (cfs). It is important to note that this pattern of minimum and peak flows may vary from year to year and can be influenced by various factors such as precipitation, temperature, and land use practices. The annual discharges (cfs) of the streams are shown in (**Table 8-1).**

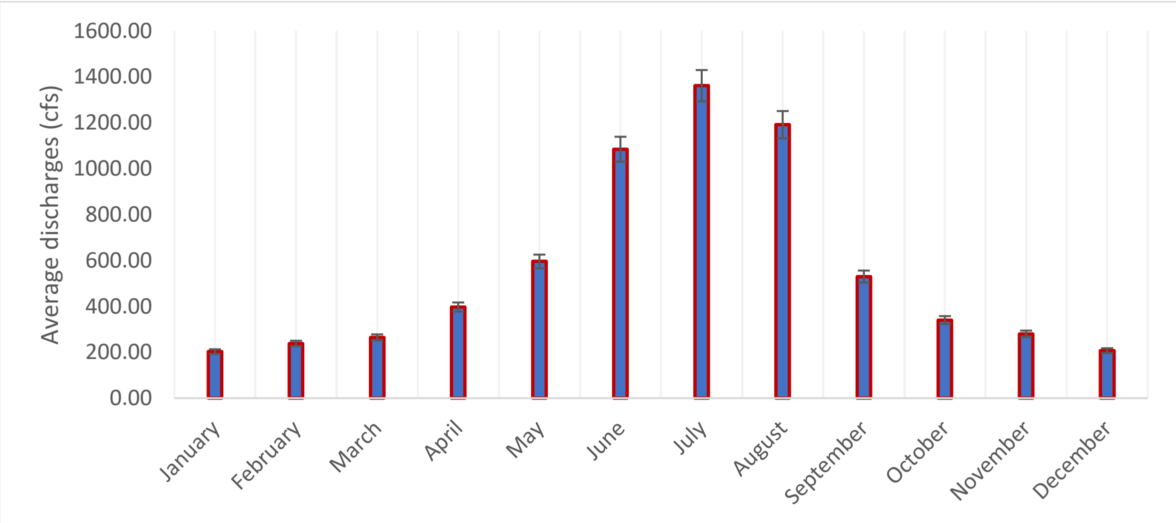

Figure 6-2: Annual flow rate in the Deh Halkani plot area discharges (cfs) (1999-2022).

The **(Figure 6-3**) shows the catchment basins and calculated discharges for the period of 1999 to 2022. The data indicates that the flow of the river increases with the passage of time, with the highest peak flow occurring in 2022. The flow rate is measured in cubic feet per second (cfs). It is important to note that the flow of a river can be influenced by various factors such as precipitation, temperature, and land use practices, and can vary from year to year. The catchment basin, is the area of land where all the water flows into a particular river or stream **(Figure 6-3)**.

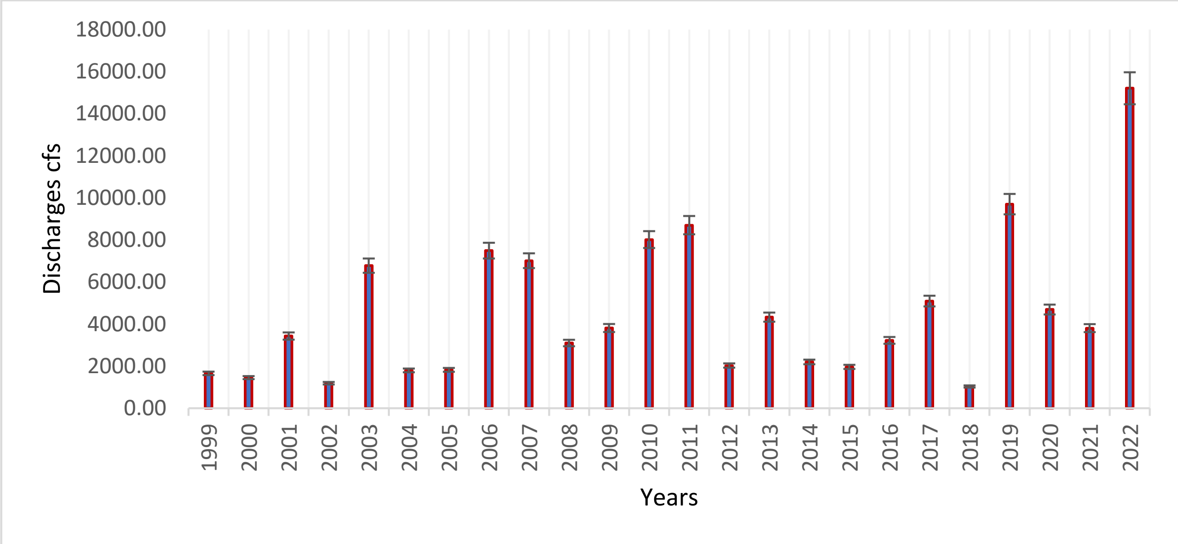

Figure 6-3: Annual Catchment basins and calculated discharges (cfs) (1999-2022).

6.2 Weather data

Thoroughly investigated all potential sources of weather data for this project. However, as mentioned in the previous section, there are no weather stations located in the region surrounding the Halkani plot and the nearest stations are quite far away. The temporal resolution of ground-based measurement is somewhat limited, and in some cases, it may not be reliable for determining the intensity of short-term rainstorms. Given the limitations of ground-based data, including the limited data range, unrepresentative gauging stations, and poor quality of the data, satellite-based data is a necessary alternative. Satellite data is available at daily and sub-daily intervals, with varying spatial resolutions.

To study the climate of the plot area and model its hydrology, we collected daily weather data from various sources such as multi-satellite measurements, reanalysis, and hydrodynamic models. The data covers the past 23 years and was obtained in order to simulate long-term hydrographs of the local streams in the plot area using the HEC-RAS model. The use of satellite-based sources was specifically chosen to provide a comprehensive view of the weather patterns in the area [3].

Satellite-based measurements and reanalysis sources provide daily and sub-daily data on a range of weather parameters such as air temperature, and rainfall depth and intensity. Calculated the average monthly and annual rainfall depth for each satellite pixel grid based on the daily data. As

[3] Solar GIS Data

shown in (**Figure 6-4**). The average annual rainfall depth in the plot area is 241 mm, with a uniform spatial distribution. According to the 23-year record of rainfall data, the highest annual rainfall depth in the plot area occurred in 2003, 2019 and 2022, with 528 mm, 235 mm and 352 mm respectively. In this region, 70% of the annual rainfall occurs during the summer season (June to August) and 30% during the cold season (September -April). A comparison of rainfall data from satellite-based models shows that the average rainfall depth in the plot area has increased by 35-45% in the last 10 years compared to the previous 10-year period.

Table 6-1: The sources, spatial and temporal resolutions of weather data for HUB river basin[4].

Data Sources	Time Period	Parameters
Solar GIS Data	1999-2022	Temperature, Rainfall, Humidity
NASA Power	1999-2022	Temperature, Rainfall, Humidity

The Halkani project plot site has experienced a trend of rising temperature variations in last 5 years. The data collected from (1999 - 2022), indicates that the summer months, particularly June, have been the warmest, while the winter months, especially January, have recorded the lowest temperatures. It is also worth noting that the temperature increases at the site between the years 1999 and 2022 have been systematically recorded. The temperature variation values mentioned in below (**Table 6-2**)

[4] NASA-Power https://power.larc.nasa.gov/#resources

Table 6-2: Temperature variation (°C) between the year (1999-2022)

Year	Jan	Feb	Mar	Apr	May	Jun	Jul	Aug	Sep	Oct	Nov	Dec	Year	
1999	19.0	22.0	24.6	28.8	30.1	30.4	29.3	28.3	28.0	28.9	25.2	20.4	26.3	1999
2000	19.2	20.6	25.0	29.0	30.2	30.3	29.5	28.5	28.0	28.0	25.0	21.2	26.2	2000
2001	19.2	22.3	25.4	27.9	30.1	30.2	29.0	28.5	28.6	28.7	25.6	22.8	26.5	2001
2002	19.7	21.0	25.9	28.6	30.3	30.7	29.0	28.1	26.9	28.8	25.2	21.3	26.3	2002
2003	20.2	22.2	25.3	29.6	29.7	30.2	29.6	28.8	28.0	28.5	23.9	20.4	26.4	2003
2004	19.4	22.3	27.1	29.2	30.4	30.6	29.2	28.3	27.9	27.6	25.4	21.7	26.6	2004
2005	18.8	20.7	25.1	28.2	29.8	31.1	29.4	28.3	29.2	28.3	25.4	20.2	26.2	2005
2006	18.6	24.0	25.1	28.0	29.7	30.2	29.5	27.9	29.3	29.1	26.1	19.9	26.4	2006
2007	19.9	22.6	24.5	28.8	30.3	31.3	30.6	29.1	29.5	28.0	25.5	19.6	26.7	2007
2008	17.7	19.4	26.0	28.1	29.4	30.9	29.4	28.5	28.9	28.6	24.6	20.3	26.0	2008
2009	20.2	22.8	26.0	28.8	31.0	31.0	30.0	29.2	28.7	28.3	24.6	21.1	26.8	2009
2010	20.0	21.4	26.7	29.0	30.8	30.1	30.2	29.2	28.9	28.5	25.4	19.8	26.7	2010
2011	19.0	21.6	25.4	28.3	29.9	30.5	29.7	29.1	28.5	27.8	26.2	20.7	26.4	2011
2012	18.7	19.8	24.5	28.4	30.1	30.0	29.4	28.6	29.3	28.4	25.7	21.0	26.2	2012
2013	19.4	21.5	25.7	28.0	30.1	31.5	29.8	28.4	28.8	29.4	25.2	20.6	26.6	2013
2014	18.0	20.8	24.7	28.1	30.2	31.5	30.0	29.2	28.9	28.6	25.6	20.5	26.4	2014
2015	19.3	22.2	24.8	29.2	30.6	32.2	29.9	28.8	29.4	29.2	25.5	20.4	26.8	2015
2016	21.0	22.4	26.0	28.1	30.3	30.9	30.1	29.2	28.4	27.8	24.8	22.5	26.8	2016
2017	18.6	22.1	25.2	28.8	30.5	31.4	29.6	29.0	28.4	29.0	24.6	20.0	26.5	2017
2018	20.5	22.6	26.3	29.1	31.6	30.9	30.0	28.4	27.7	28.7	26.1	20.5	26.9	2018
2019	19.4	20.6	24.4	28.4	30.1	31.9	30.6	29.1	30.1	29.0	24.8	19.6	26.5	2019
2020	17.5	22.2	24.3	28.7	30.5	31.7	31.9	30.4	30.0	29.0	23.4	19.6	26.6	2020
2021	17.9	22.9	26.5	29.5	31.3	31.1	30.4	28.7	30.7	27.8	25.1	20.0	26.8	2021
2022	18.0	22.3	26.7	29.3	30.2	30.3	29.3	28.8	28.9	28.0	24.9	--	--	2022
LTA	19.2	21.7	25.4	28.6	30.3	30.9	29.8	28.8	28.8	28.5	25.2	20.6	**26.5**	

Unit: **°C** Long-term statistics is calculated from complete years Yearly STDEV: 0.2 °C

The Halkani plot area has recorded rainfall data over the last 23 years, from (1999-2022). The precipitation data collected over this period provides a comprehensive view of the rainfall patterns at the site. According to the data, the years 2003, 2010, and 2011 have recorded the highest average annual rainfall. Furthermore, it is noted that the peak maximum rainfall occurred during the year 2022. Additionally, an increasing trend in the rainfall pattern over the past 23 years can be observed from the data. The rainfall variation is illustrated in the graph depicted in (**Figure 6-4**).

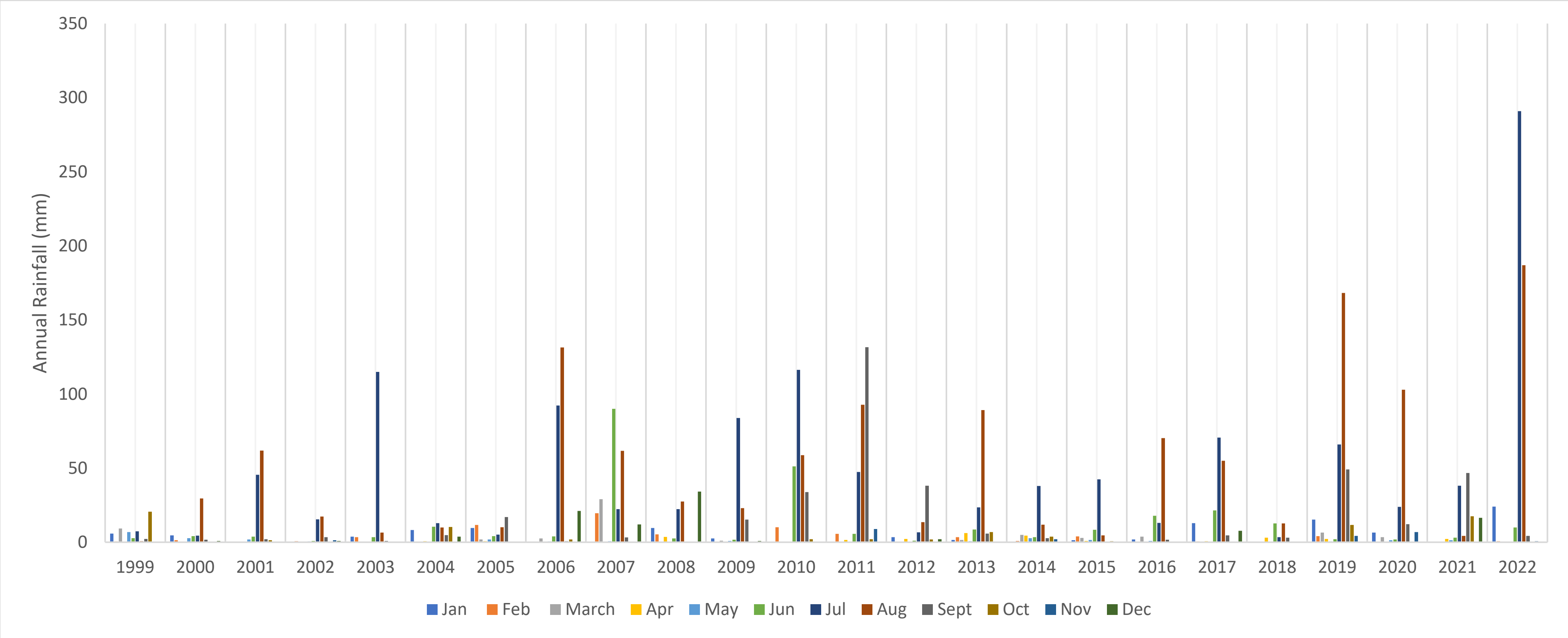

Figure 6-4: Long-term Rainfall pattern(mm) at Halkani plot area (1999-2022).

6.3 Topographic Data

The Shuttle Radar Topographic Mission (SRTM) digital elevation model are used for terrain modelling of the project site with the help of ground topographic survey data. Topographic data is readily available in a variety of spatial resolutions, with the most common choice for medium scale hydrological modeling being SRTM-30, a digital elevation model with a spatial resolution of 30 meters. For this study, we used a DEM collected by the Phased Array Type L-Band Synthetic Aperture Radar instrument of the Advanced Land Observing Satellite (SRTM-30 meter). The SRTM data 30-meter resolutions, both of which are freely available to a wider community of users. The DEM of the plot area was processed to fill in gaps and then used in the modeling phase. (**Figure 7-1**) a 3D view of the Halkani plot area. To visualize the topographic conditions of the surrounding areas, DEMs of those areas are also shown in **(Figure 6-5**). Please note that the topographic data was provided by STS Consulting in TIN and ESRI Shapefile format. However, for hydrological modeling, topographic data of adjacent areas is also required. Therefore, we used data downloaded from SRTM for this purpose.

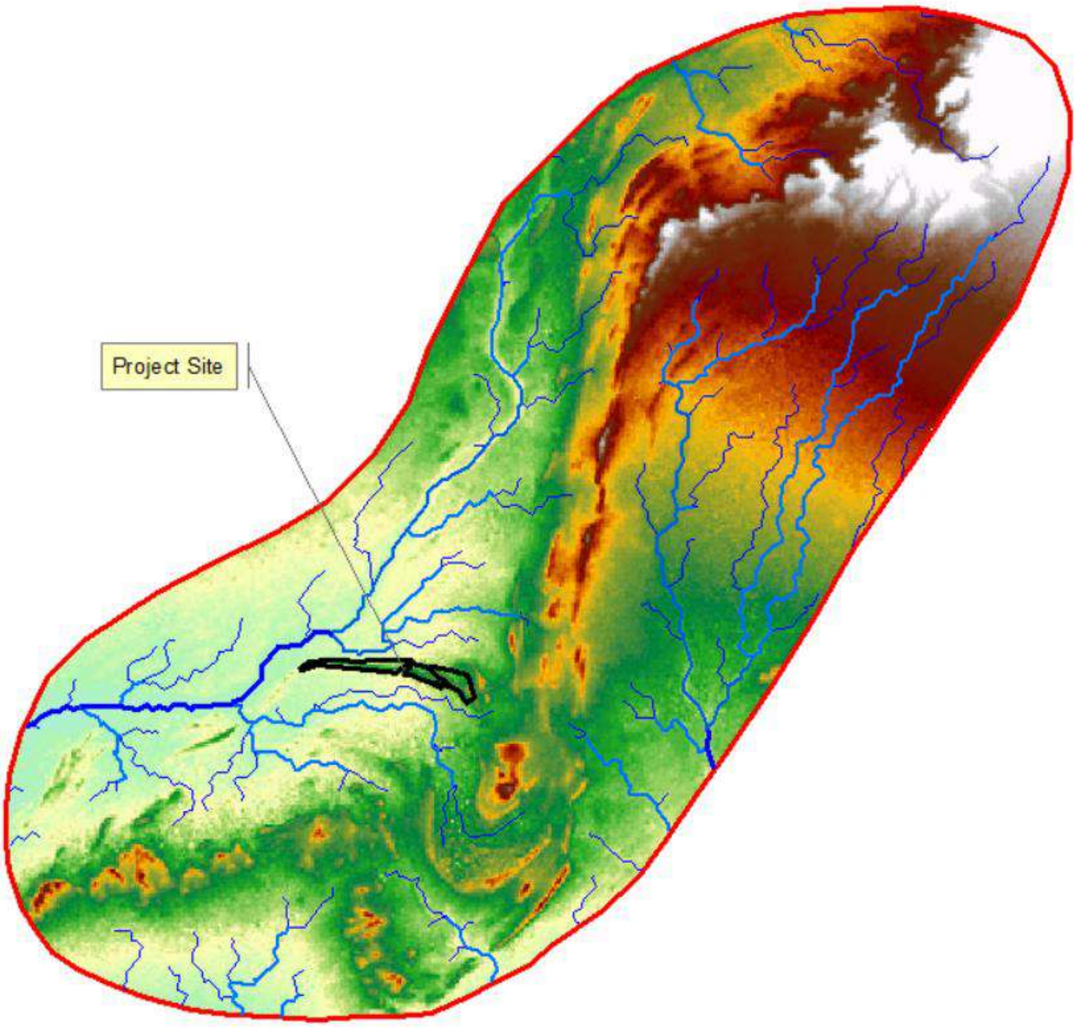

Figure 6-5: DEM of the Halkani plot site and adjacent areas.

The topographic survey of project area was used out for hydrological studies and modeling. To assure the quality, the data has been verified from satellite imagery and GIS technology. After collecting detailed topographic information, the 3D modeling analysis is carried out to have a better understanding of the hydrographic variations in the project area. A detailed topographic map is attached in Annex B.

3D models are generated for whole area shown in (**Figure 6-5).** Stream flows are also represented on the same 3D model. For further explanation and understanding, aerial 3D model of study area, hydrological flow accumulation behavior of watershed, flow direction behavior of the study area and overall elevation of the area are presented and shown in below sections of this report.

6.4 Land use and Landcover Data

A land use map of the plot area and its surroundings shown in (**Figure 6-6**) was obtained and modified for use in hydrologic modeling. This data layer serves as input for both hydrological and rainfall-runoff models. The land use in the plot area and its surroundings is primarily winter pasture, with some agricultural use. Due to the sub-arid climate conditions, the terrain is prone to significant erosion. The land use classes and runoff coefficient constant values used for HEC-RAS model are depicted in (**Table 6-1**).

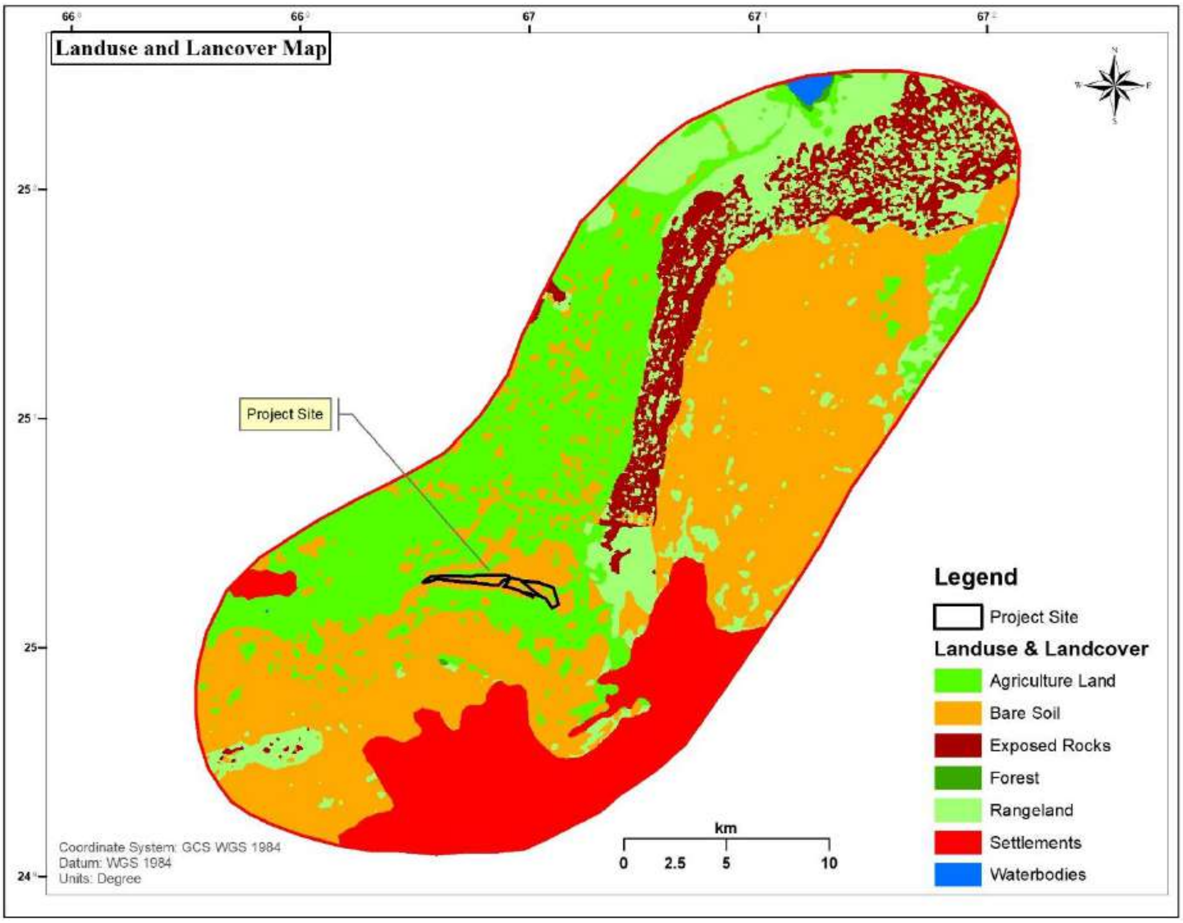

Figure 6-6: The Land use map of the plot site and surroundings.

Table 6-3: The landuse classes and runoff coeffiecent cosntant values for HEC-RAS model.

S. No	Land Use Classes	Run-off Coefficient Constant 'C'
1	Open Space	0.19
2	Forest	0.14
3	Settlements	0.32
4	Bare soil	0.08
5	Rangelands	0.035
6	Agricultural	0.03
7	Barren	0.035
8	Waterbodies	0.02

6.5 Slope data

The slope analysis of the Deh Halkani plot and its surroundings (**Figure 6-7**) indicates that the majority of the area has moderate and gradual slopes, with elevations ranging from 16 to 24 meters. However, the adjacent area of the project plot features significantly steeper slopes, with inclinations ranging from 62 to 100 meters. The sloping terrain reduces the likelihood of rainwater accumulation but increases the risk of soil erosion during heavy rain seasons. To address this, land leveling and adequate drainage systems are crucial in the lower areas of the project plot to mitigate soil erosion. The slope rate is used as input for the HEC-RAS model, which simulates flood inundation, flood velocities, and generates flood profiles.

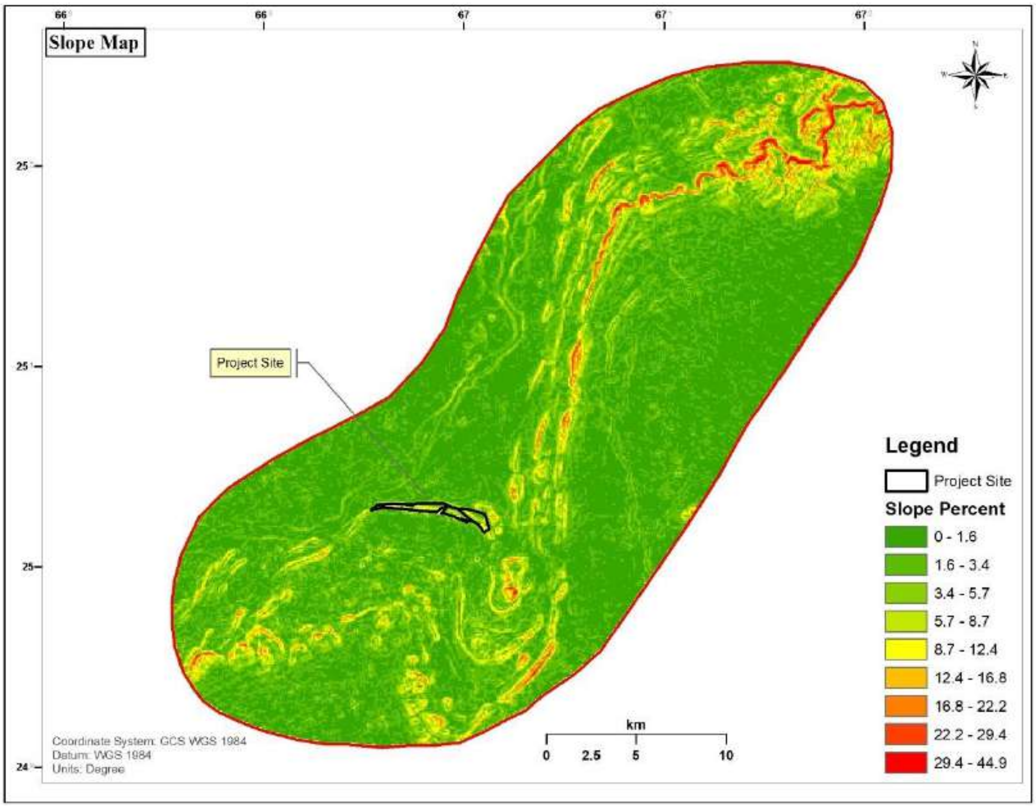

Figure 6-7: The slope map of the plot site and adjacent areas.

7 WATERSHED ANALYSIS HYDROLOGICAL AND HEC-RAS MODELLING

7.1 Data preparation for model (HEC-RAS Model Preprocessing)

The preprocessing of fictitious data for the HEC-RAS model in a GIS environment is accomplished by using the HEC-GeoRAS extension. It is appropriate to combine HEC-RAS with GIS Software for the torrent flood zoning model [1]. Using evaluation digital models of the earth's surface and performing 3-Dimensional analyses in ArcGIS environment are very useful to extract the necessary data of HEC-RAS model. The SRTM digital elevation model (DEM) was employed to generate Triangular Irregular Networks (TINs) of the adjacent areas of the project. A Triangulated Irregular Network (TIN) is a method of representing a continuous surface using a network of triangular facets, also known as a triangle mesh. It is primarily used as a Discrete Global Grid give a clear slopes and elevation of ground surface which is illusrtaed in (**Figure 7-1**).

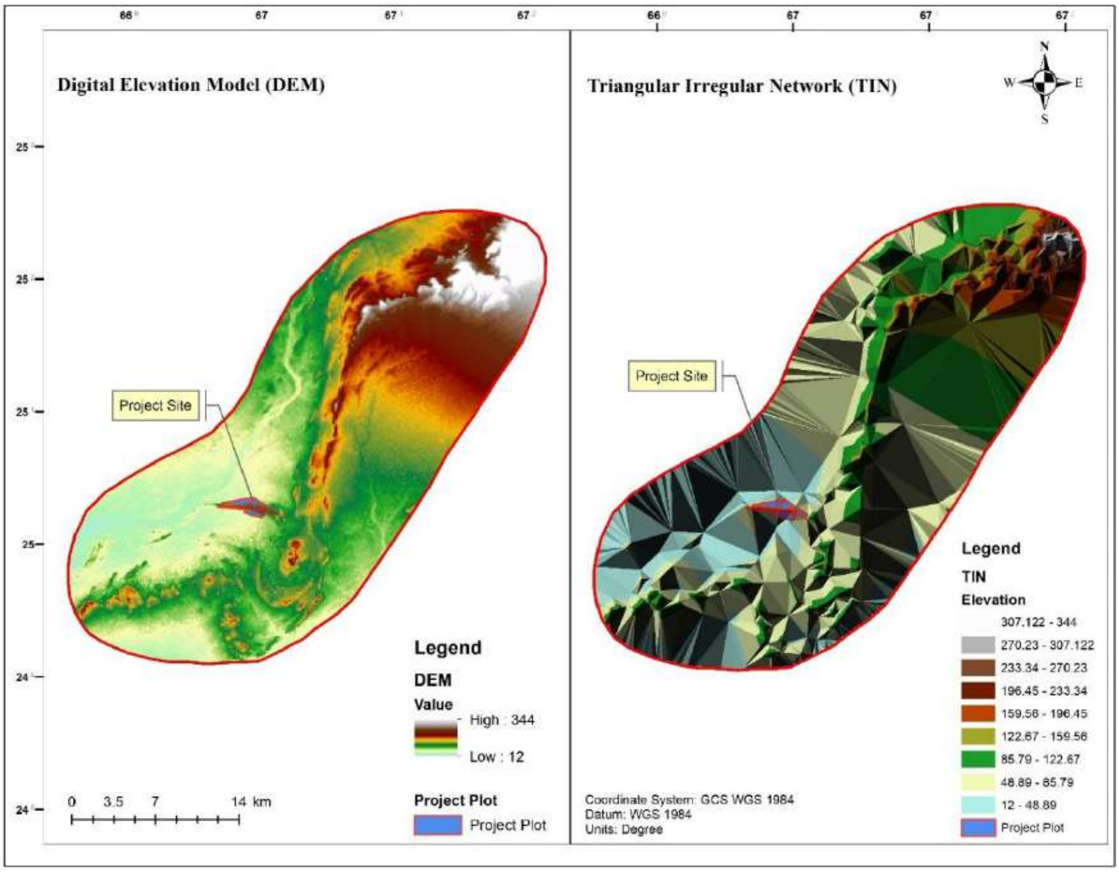

Figure 7-1: The Digital Elevation Model and Triangular Irregular Network (TIN) of project area

A preliminary database was constructed in ArcGIS using the HEC-GeoRAS extension, utilizing the SRTM (TIN) as the basemap and slope data. The main channel and interlinked tributaries were identified and the data was subsequently exported to generate the necessary geometry file for the HEC-RAS models. HEC-RAS model require high precision and accurate data set, thus this process will provide a reliable set of data for the simulation of flood and hydrology.

In the subsequent section of the report, a comprehensive explanation of the compiled data inputs for the HEC-RAS models is provided. These inputs include:

1. Main channel and tributaries (HUB-River)
2. Banks of the main channel
3. Flow pathways
4. XS cut lines (Cross-sections of the channel)
5. Manning's values (derived from Landuse and land cover data)

The input layers that are necessary for the task, as shown in the **(Figure 7-2)** below, were created using ArcGIS software.

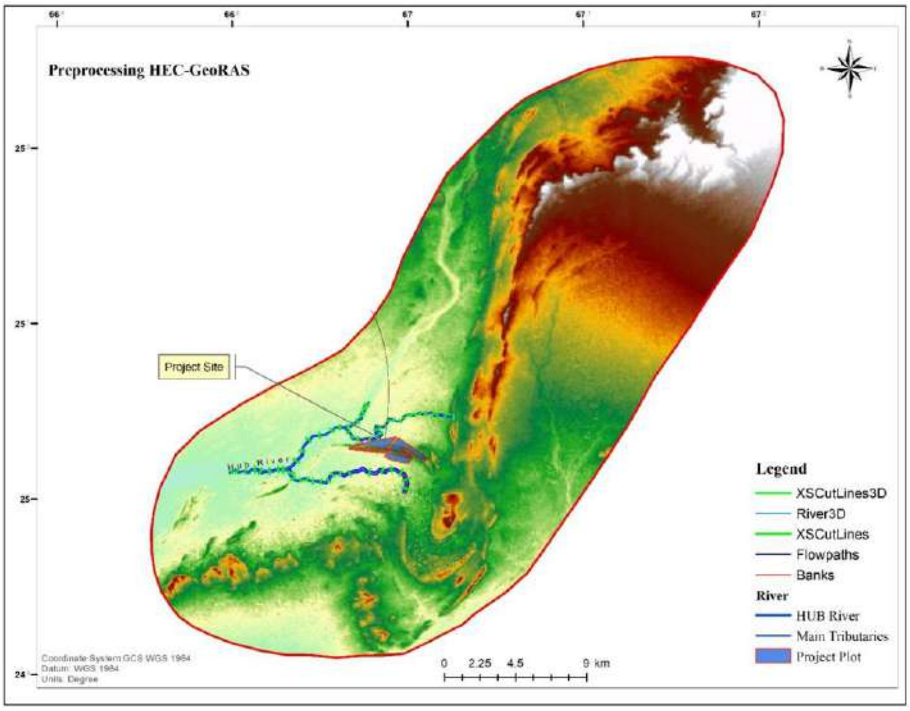

Figure 7-2: Preprocessing data layers for HEC-RAS model

1. Main channel and tributaries

The stream network in the vicinity of the project site was identified through the process of stream identification and watershed delineation. This involves extracting both perennial streams, which are those that flow year-round, as well as ephemeral streams, which are streams that only flow during periods of heavy rainfall. The primary channel in the area is the HUB River, which is located approximately 2 km from the project plot. Additionally, there are number of small tributaries in the surrounding area, which provide significant inflow to the main channel during rainy seasons. These tributaries are also extracted for the HEC-RAS model as they play an important role in the runoff, flood and erosion analysis in the study area. The HEC-RAS model uses these inputs to simulate the river flow, water surface elevations, and water velocities, and it outputs information such as water levels, flood extents and other key parameters that can be used to evaluate the effect of the project on the river system. The primary channel, the HUB River, and its main tributaries have been plotted and are depicted in (**Figure 7-2).**

2. Banks of the River and Tributaries

The HEC-GeoRAS extension was utilized to digitize the banks of the primary channel, the HUB River, and its main tributaries. This process involves the creation of a digital representation of the river banks using a triangular irregular network (TIN) model. This model uses the elevation data of the area to generate a representation of the topography, which is then used to define the banks of the river. The TIN model allows for accurate representation of the riverbanks, including the locations of meanders and changes in river width. The Banks of the channel (HUB River) and its main tributaries have been plotted and are represented in (**Figure 7-2**).

The main channel and its main tributaries are identified on the basis of the flow throughout the year and its maximum extent that it covers. This is important for the HEC-RAS model as it is used to simulate the river flow and to understand the extent of floods and erosion. The digital representation of the river banks created by the HEC-GeoRAS extension is then used as input for the HEC-RAS model, which can accurately simulate the flow of water in the river and provide information such as water levels, flood extents, and other key parameters that are used to evaluate the impact of the project on the river system.

3. Flow pathways

Flow Path lines are used to compute reach lengths between cross sections in the left and right over bank. Flow path lines are created in the downstream direction following the center-of-mass of flow in the left and right overbanks. Flow Path lines are used to identify the key pathways that water takes as it flows through a catchment. This information is then used to understand the distribution of water within the catchment and how it might change over time in response to changes in precipitation and discharge. These lines are also used to estimate the water discharge from the catchment area and how it varies with time. Additionally, to identify the areas that are more prone to flooding, and also helps in identifying the locations for the construction of flood control structures. The flow pathways of the channel (HUB River) and its main tributaries have been plotted and are represented in **(Figure 7-2).**

4. XS Cut Lines (Cross section of the channel)

The cross-sections are used to obtain elevation data from the terrain to create a ground profile of the channel flow. This profile provides information about the shape of the channel and the elevation of the riverbed at different locations.

The cross-sections are used to represent the channel geometry and topography, which is an important input for the HEC-RAS model. The model uses this information to simulate the flow of water in the channel and predict water levels, velocities, and flood extents. The cross-sections also provide information about the width, depth and slope of the channel which is important for the computation of discharge and other hydrological parameters. The cross-sections of the HUB River and its main tributaries have been plotted and are represented in **(Figure 7-2).**

5. Manning's values (Land use and landcover data)

The Manning's n value is a dimensionless coefficient that represents the roughness or friction factor of a conduit. This coefficient is used to quantify the resistance to flow in channels and floodplains. The Manning's n value is a measure of the roughness of the channel's bottom and sides, and it considers the physical characteristics of the channel such as the surface roughness, vegetation, and other LULC features illustrated in **(Figure 6-6).** In HEC-RAS, the Manning's n value is used as an input to the model to simulate the flow of water in a channel. The model uses the Manning's n value to calculate the frictional resistance of the flow, which affects the velocity of the flow and the water level in the channel. The coefficient value against each land use and landcover class are present in **(Table 6-1).**

7.2 Watershed Analysis and Simulation Model of Daily Discharges of the Hub River

A watershed analysis was conducted on not only the plot area, but also the entire adjacent areas to visually depict the stream network and potential areas of water accumulation. A Digital Elevation Model (DEM) with a spatial resolution of 30 meters was used for the analysis. The total area included in the analysis was greater than 7,000 km² **(Figure 7-3).** In addition, to depict local watersheds in greater detail within the plot area, sub-basins were also considered in the analysis. The total area of the sub-basins analyzed was 4500 km².

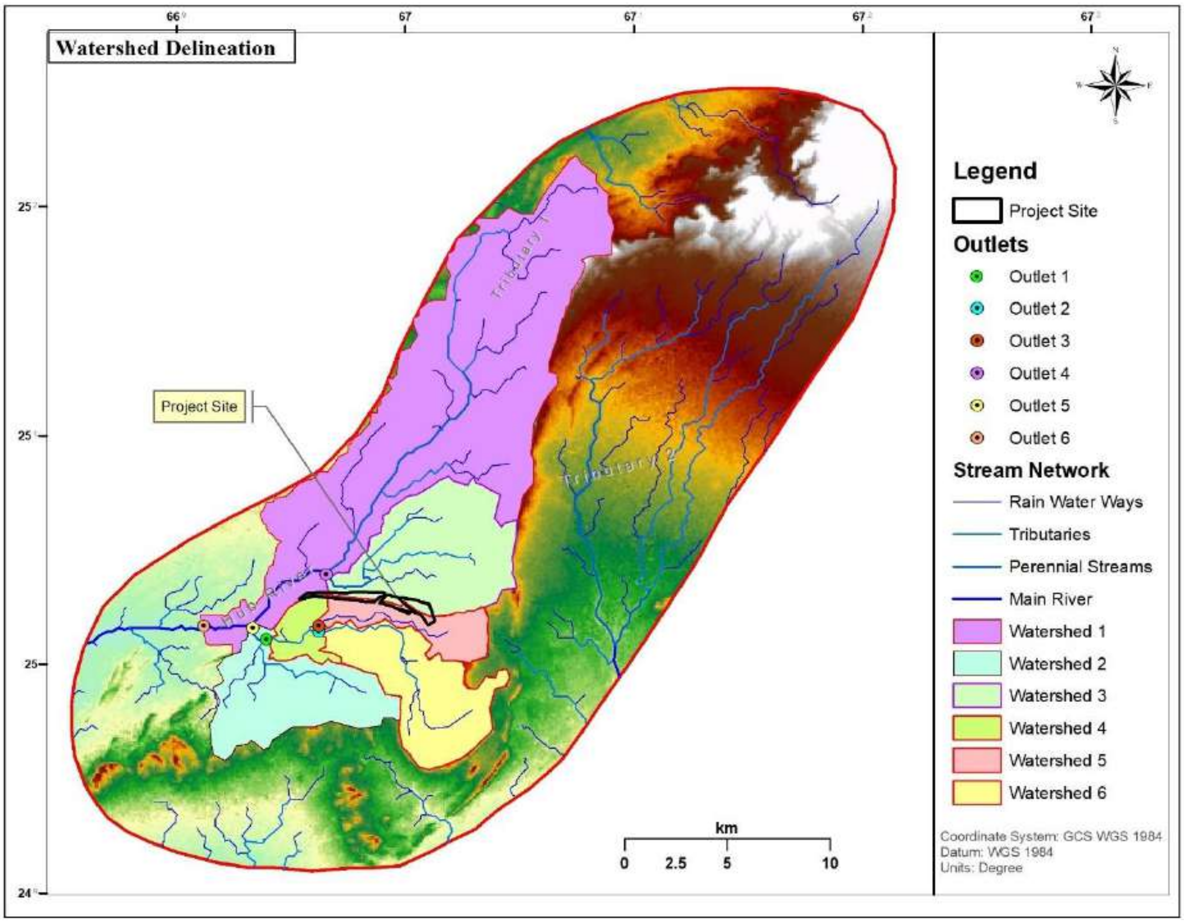

Figure 7-3: Watershed basin included plot area

As previously stated, no hydrometric measurements were conducted on the rivers within the plot site. Due to the lack of discharge or flood event data on these small streams, average and flood discharges were calculated using traditional methods outlined in Section 7.1. This approach allowed for the characterization of the flow patterns of these streams. However, it is challenging to extract peak discharges and flood events from this data. As such, special emphasis was placed on simulating long-term discharges and potential flood events using available techniques [2].

7.3 Post Processing of (HEC-RAS Model)

Post-processing in HEC-RAS involves analyzing and interpreting the results of a hydraulic model simulation. The simulation is based on the constructed data imported from HEC-GeoRAS extensions and uses dynamic routing to calculate 2D-dimensional steady flow in a full network of reconstructed channels. After a new project was created in the HEC-RAS software, the previously generated geometrical data from HEC-Geo RAS was imported and utilized in the simulation. The imported data included a schematic representation of the river and detailed cross-sectional information at key junctions [3]. This information is essential for accurately simulating the river's flow dynamics. The geometrical information for each cross-section includes the section number, river name, and the area of the section, alignment station points and their elevations, the internal length downstream, Manning's roughness coefficient, the main channel HUB river Station, and the convergence and divergence coefficients. These parameters are used to calculate the flow velocity, discharge, and water surface elevation at each cross-section, providing a comprehensive analysis of the river's hydraulic characteristics

7.4 Geometric Data processing

The GIS format data, imported into the HEC-RAS model, has been successfully integrated. The main channel and tributary bank stations are active, as shown in **(Figure 6-4).** Additionally, the river's details are illustrated in the **(Figure 7-5).** The Manning's values and cross-sections of the river has been verified and the residual errors has been eliminated prior to running the model [4].

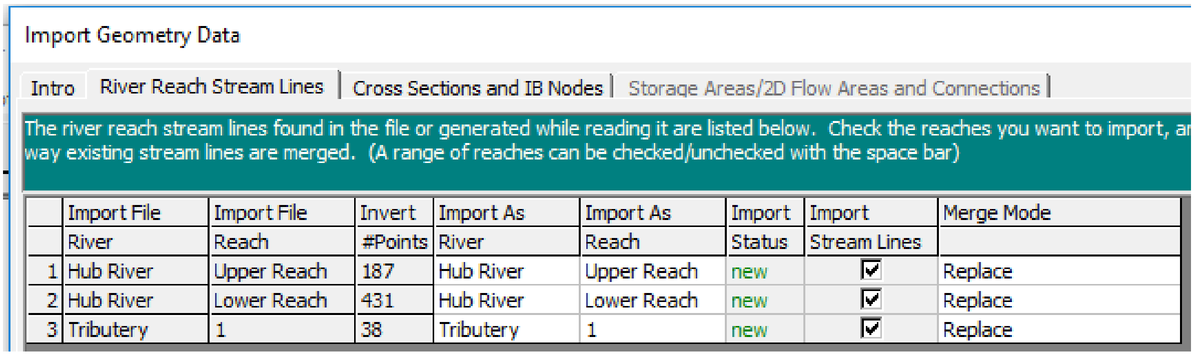

	Import File River	Import File Reach	Invert #Points	Import As River	Import As Reach	Import Status	Import Stream Lines	Merge Mode
1	Hub River	Upper Reach	187	Hub River	Upper Reach	new	☑	Replace
2	Hub River	Lower Reach	431	Hub River	Lower Reach	new	☑	Replace
3	Tributery	1	38	Tributery	1	new	☑	Replace

Figure 7-4: Imported Geometry data profile in HEC-RAS

The HUB river and its main tributaries are depicted in the **(Figure 7-5).** The cross-sectional profile line represents the values obtained from the given ground data (TIN) and manning's. It also shows the upper and lower reaches of the river and its adjacent tributaries.

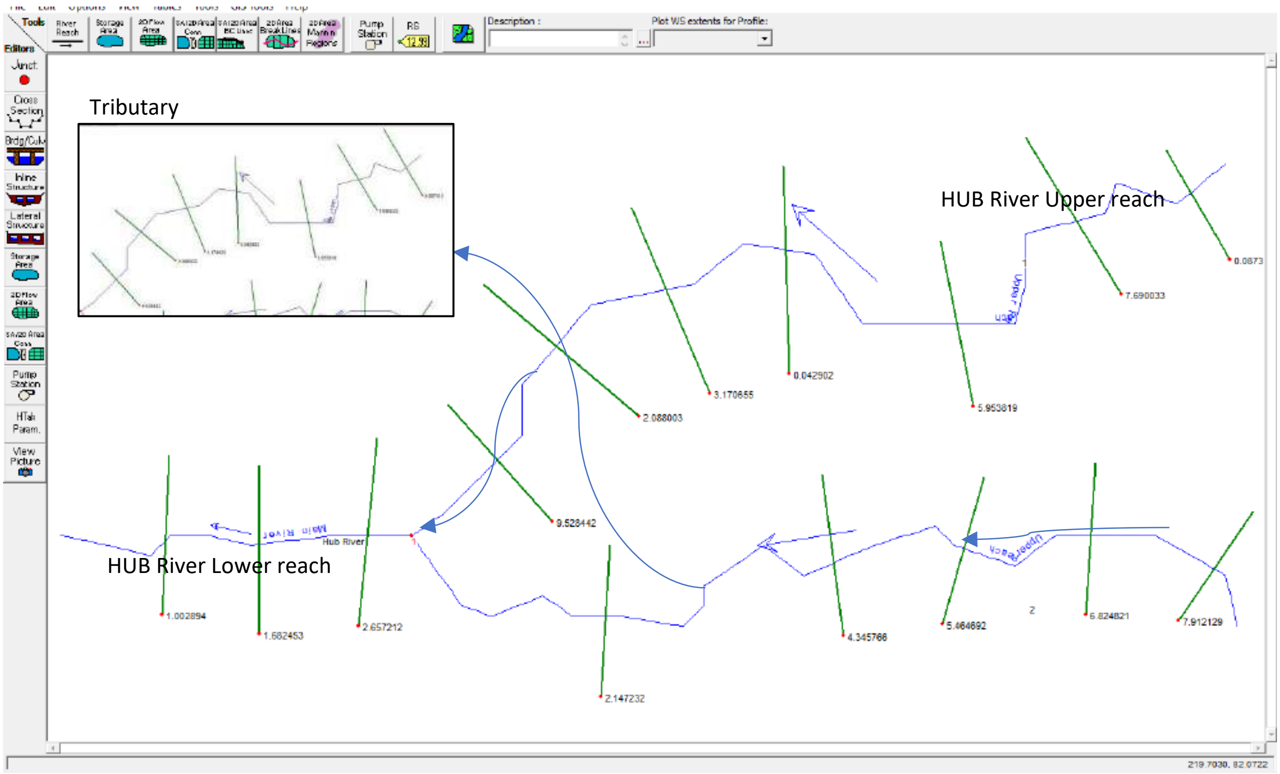

Figure 7-5: The schematic representation of HUB river and its tributaries in HEC-RAS

The cross-section of the Hub River and its tributaries are plotted and verified using the HEC-RAS model. The ground profile of the water channel is extracted by using a Triangulated Irregular Network (TIN) as input for the HEC-RAS model. This method is considered to be more reliable for remote river profiling. The combined cross-section of both the tributaries and the Hub River is approximately 110 shown in (**Figure 7-5).** The crossection profile and values extracted by model as per provided (TIN) data are ilustrated in **(Figure 7-6).**

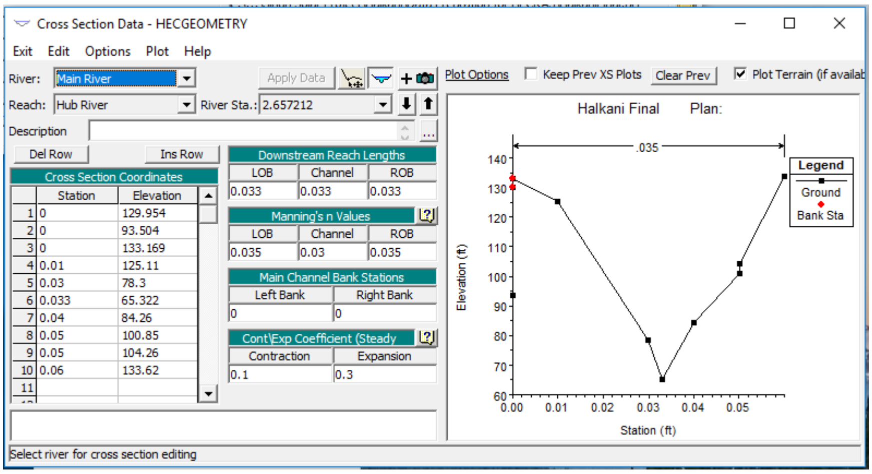

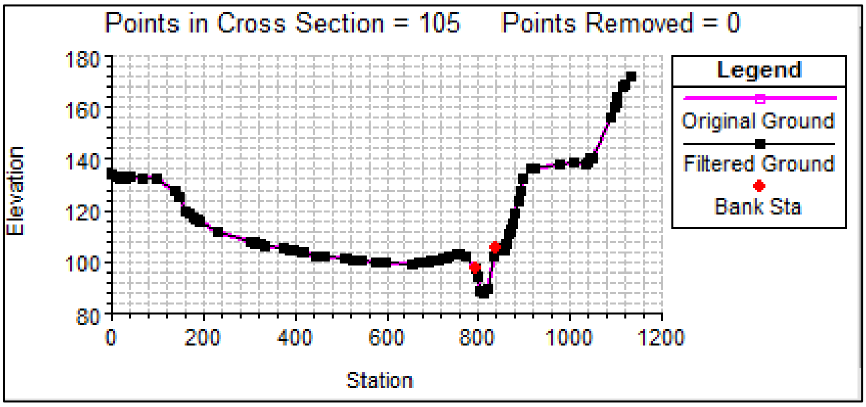

Figure 7-6: Imported Geometry data profile in HEC-RAS

The cross-section filter is utilized to verify the validity of the cross-sectional cutlines along the channel. The horizontal and vertical filter tolerances are established based on the provided ground data and any residual errors are minimized in order to prepare the data for model simulations. The cross-section filter helps to ensure that the cross-sectional data that is used in the model is accurate, and by setting the filter tolerance values according to the provided ground data, it enhance the ability of the model to simulate the river flow conditions as accurately as possible. The cross section filter profile in shown in **(Figure 7-7).**

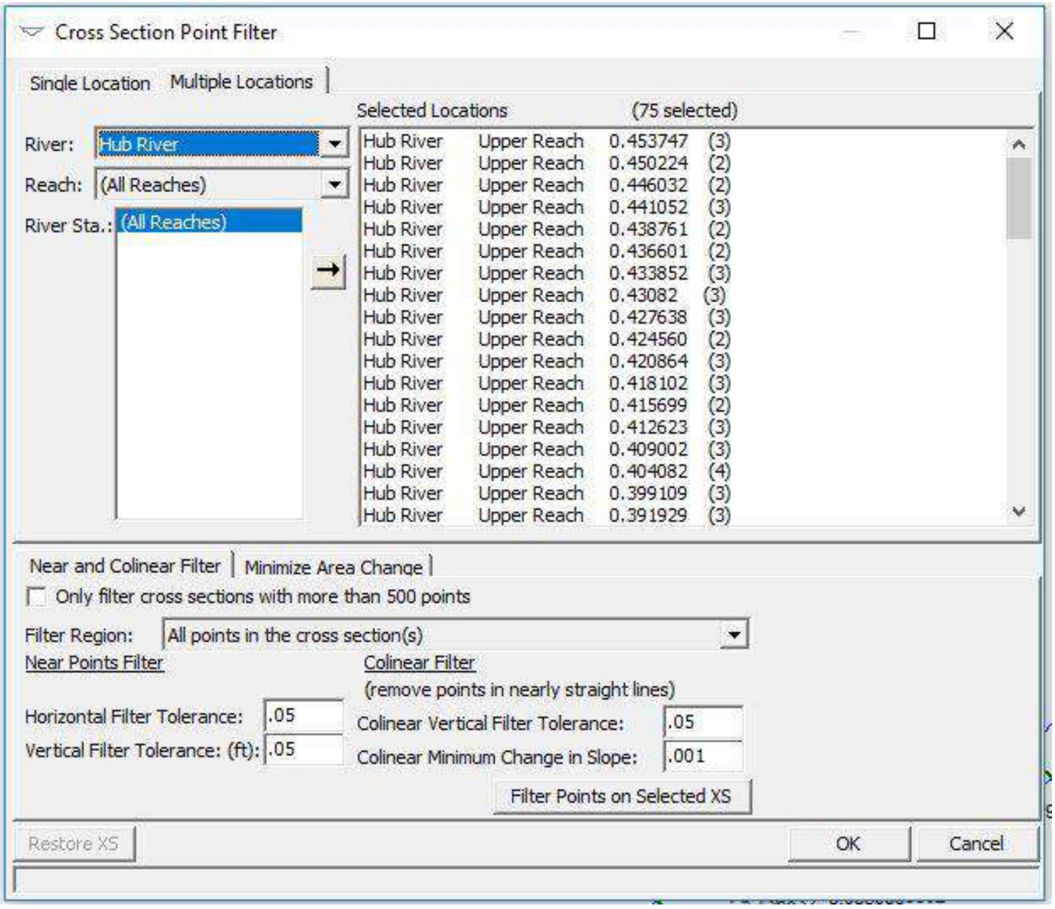

Figure 7-7: Cross section point filter

The steady flow boundary conditions refer to when the flow rate and water surface elevation remain constant at a specific location along the river or channel being modeled. The "Critical Depth" option under the "Flow Type" is used to define the boundary conditions for a particular reach or reach segment. This option allows to specify a critical depth value, which represents the minimum water depth at which the flow is considered to be supercritical, meaning the water surface elevation is above the critical depth. The critical depth value is used to calculate the flow rate and water surface elevation for that reach or segment. The critical depth for the upper and lower reach of the HUB river are set as constants. The steady flow boundary condition for the channel and assigning the critical depth shown in (**Figure 7-8).** The data for a steady, ongoing stream includes information such as the number of calculated profiles, peak stream data, and boundary conditions. Additionally, the necessary hydrological data were obtained from traditional methods outlined in the hydrology section.

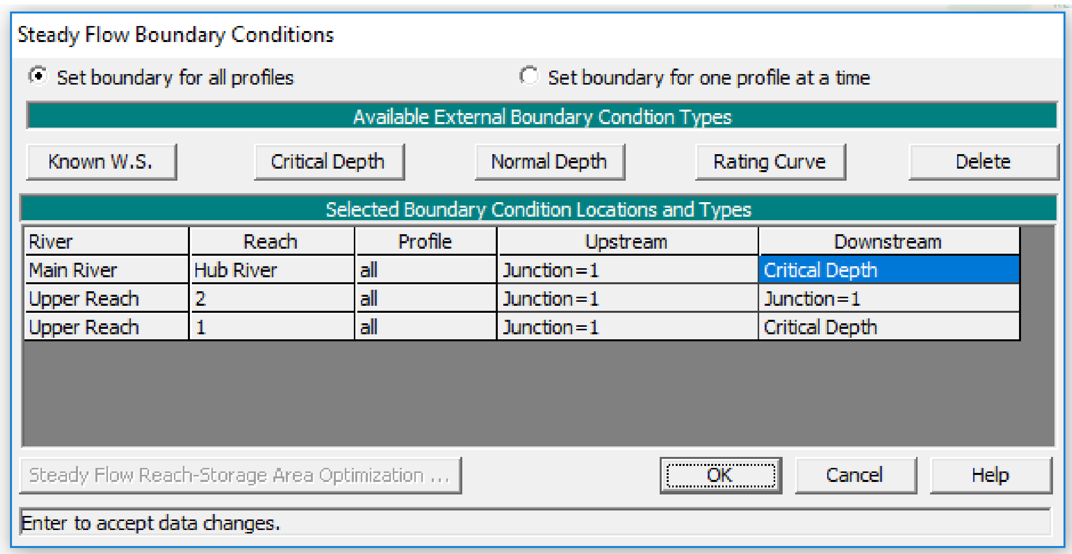

Figure 7-8: Steady flow boundary conditions

Having entered the geometrical data, the data of the flood can be entered based on it whether the stream is steady, or unsteady; then, the related hydrological data will be different. In this study, due to the river conditions, determining the river bed limit, and the river privacy, the stream analysis will be permanent; so, the resulted hydrological data of the steady stream will be entered.The flow profiles of a stream are determined using data collected over the period (1999-2022). The maximum peak flow and discharge are calculated using discharge data, and three distinct profiles are generated. These profiles consider the maximum peak flow, average flow, and minimum flow, beside the peak flow of tributaries. However, the water inundation of the river and its tributaries are modeled based on input conditions. The numbers of the calculated profiles were determined based on calculated discharge of the stream shown in (**Figure 7-9).**

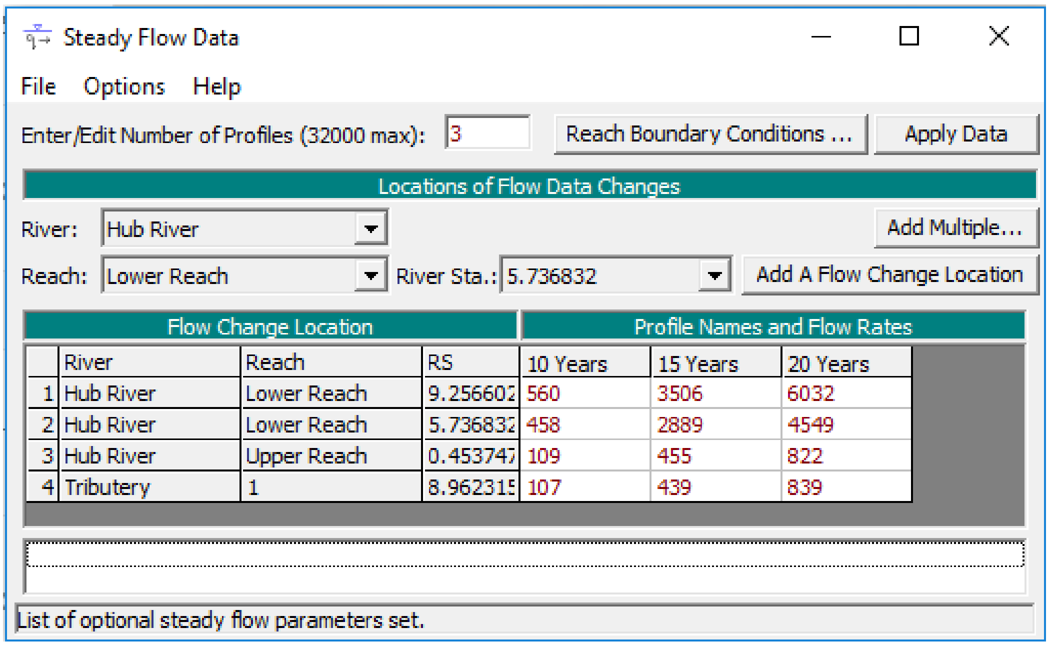

Figure 7-9: Flow change location and Steady flow data

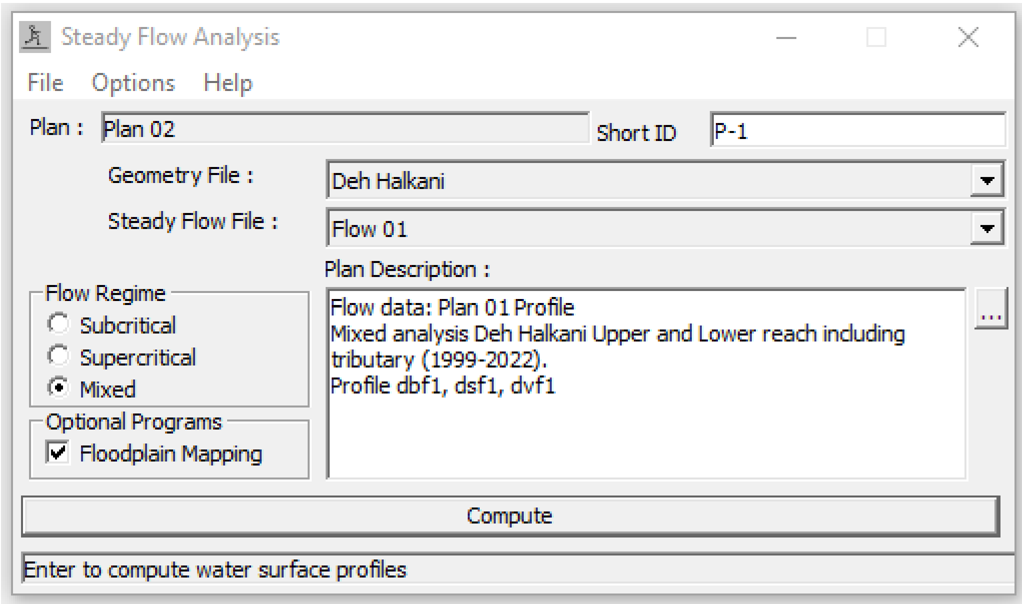

Figure 7-10: Study flow analysis of Deh Halkani site

7.5 The model calibration and validation

The model calibration and validationare are the most important factors of applying the physical, and the arithmetic models to simulate the study phenomena. The calibration is performed based on the measured data, the definite conditions of the environment, and the conformity of the variable coefficients in the model so that the corresponding conditions are created in the model. In fact, in the calibration step some of the factors are reclaimed so that the calculated digitals by the model and the measured digitals will be in conformity. Of the parameters that should be calibrated in the model is the roughness coefficient of the bed resistance in order for the stream parameters such as its depth. Finally, after additional steps, the flood water zoning for different flow and discharge rates is calculated. The arithmetic calculated values for discharge and the values calculated by the model are verified to minimize residual errors.

To enter the characteristics quantities of the river cross-sections, estimated Manning's roughness coefficient of the river were entered in to the model. Then, having entered peak stream quantities of the river floodwater, and defining its boundary conditions, the appointed model was separately run for available paths in the different hydrological condition **(Figure 7-11)** represents a sample.

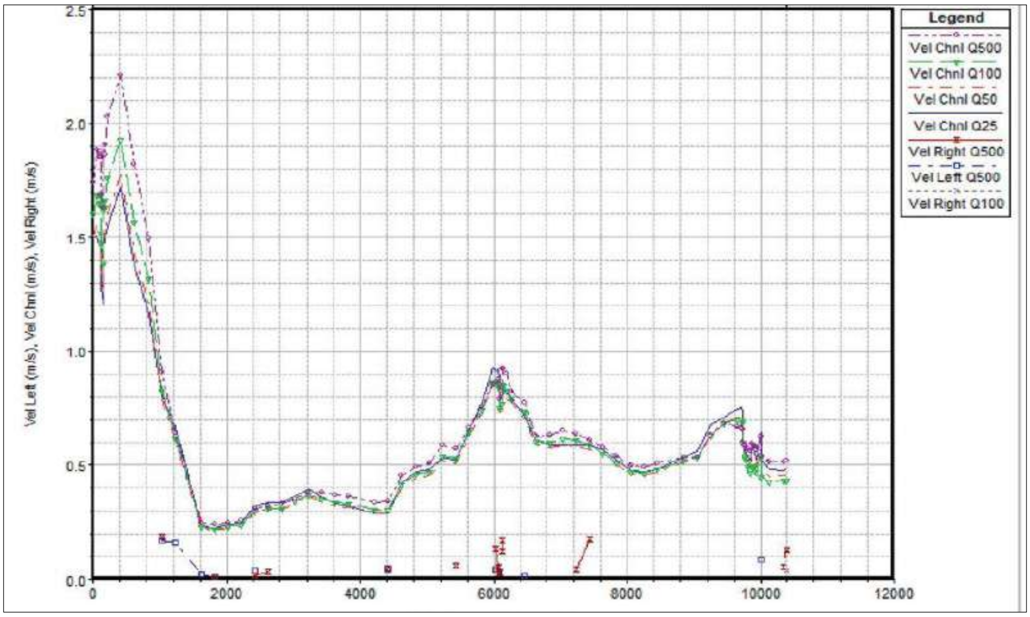

Figure 7-11: calculated velocities of model at Deh Halkani stream outlet

The final model computation of the model the flood inundation zones across the rivers are carried out. The flood velocities, stress and bank points are calculated. However, the bounding polygon and mask are covered the flood peak regions. The output of the HEC-RAS model outputs is further analyzed in ArcGIS. The flood water flow within the bank and the peak discharge of the river profile are calculated including (d-PF1, b-PF-1, s-PF-1, and v-PF-1). The inundation of all mentioned profile are further discussed in below section of the report.

7.6 Hydrology and Flood Inundation Modeling Outputs HEC-RAS

7.6.1 HEC-RAS model Flood Inundation output Layers

The HEC-RAS model is used to identify the flood inundation area along a stream by outputting different flow rates, as shown in the (**Figure 7-12).** The figure also includes a mask and bounding polygon, which illustrates the maximum flood extent during peak flows of the stream. Additionally, the model calculates the stress and velocities of the stream, as represented by the discharge profile also shown in the **(Figure 7-12)** In the ArcGIS environment, a number of profiles are created to further specify the flood extent along the stream, as explained in a later section of the report.

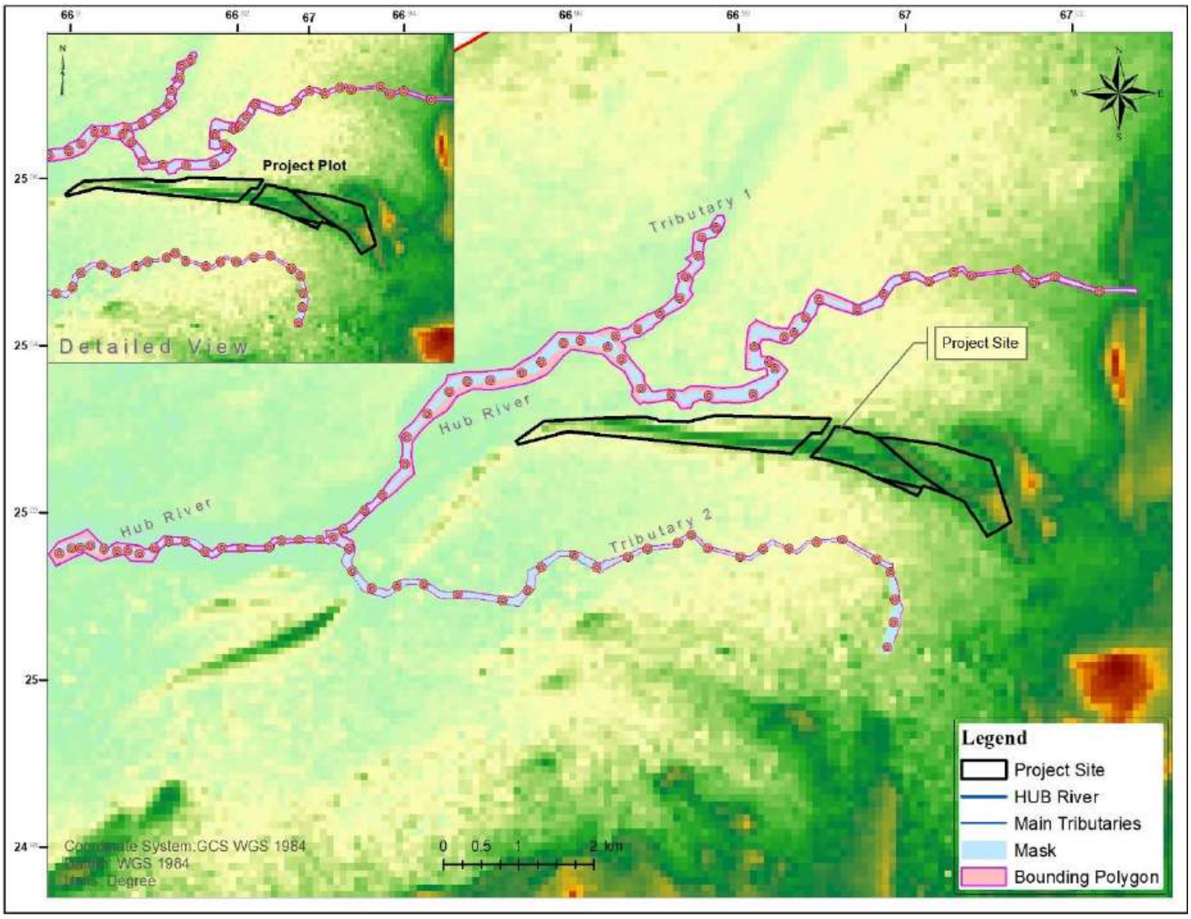

Figure 7-12: HEC-RAS model flood inundation outputs

7.6.2 Flood Inundation proile (v PF 1)

The HEC-RAS model outputs were used to generate a velocities profile, as shown in **(Figure 7-13).** This profile includes calculations for the peak flow of the stream and its velocities against the gradient. The parameters used to calculate the velocities include the resistance factors such as the existing stream bed conditions, slopes, and land use and land cover of the stream area. The model velocities are determined based on the conditions provided to the model simulations.

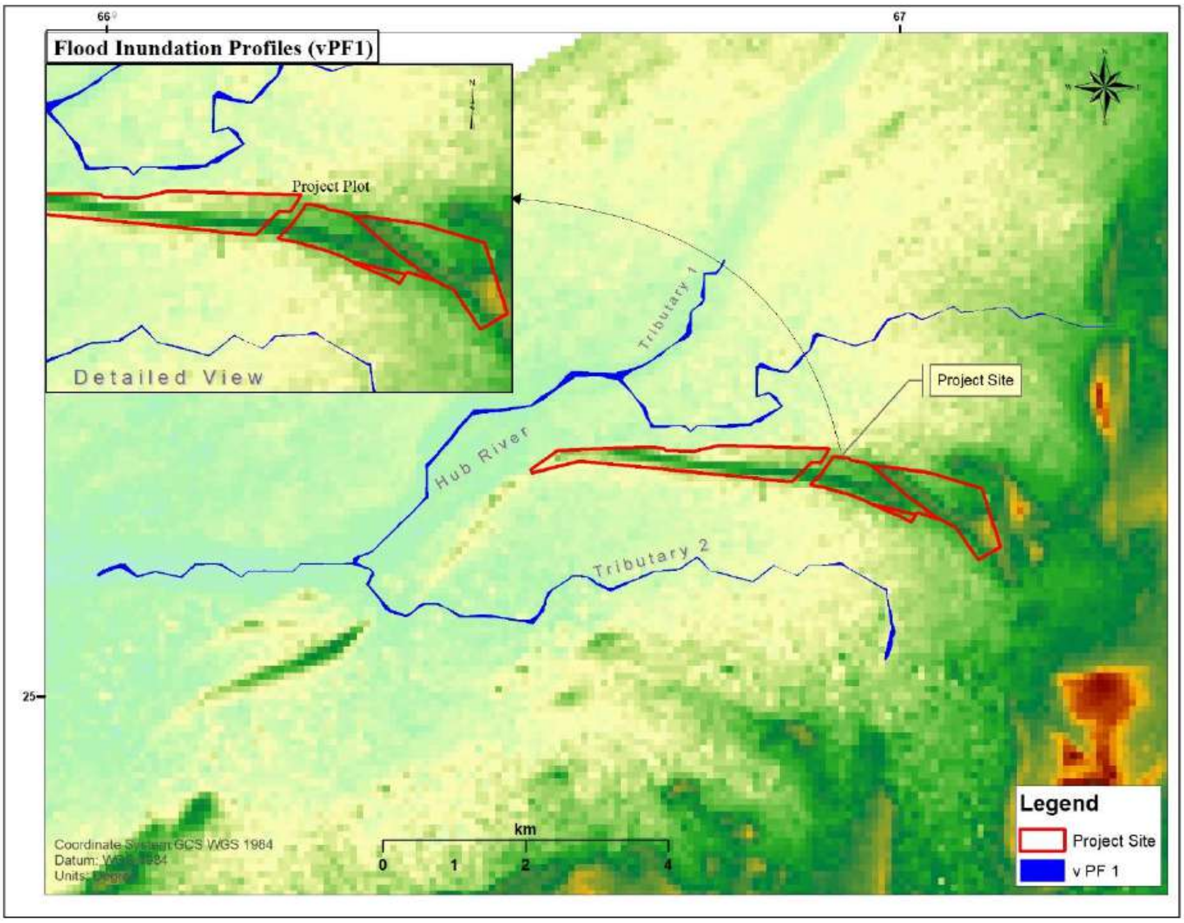

Figure 7-13: HEC-RAS model discharge profile v PF 1

7.6.3 Flood Inundation Proile (b PF 1)

The HEC-RAS model generates a base flow (b PF 1) of the stream, as shown in the (**Figure 7-14).** The maximum flow of the stream during peak flood inundates the existing banks of the stream. The (b PF 1) includes calculations for the peak flow of the stream.

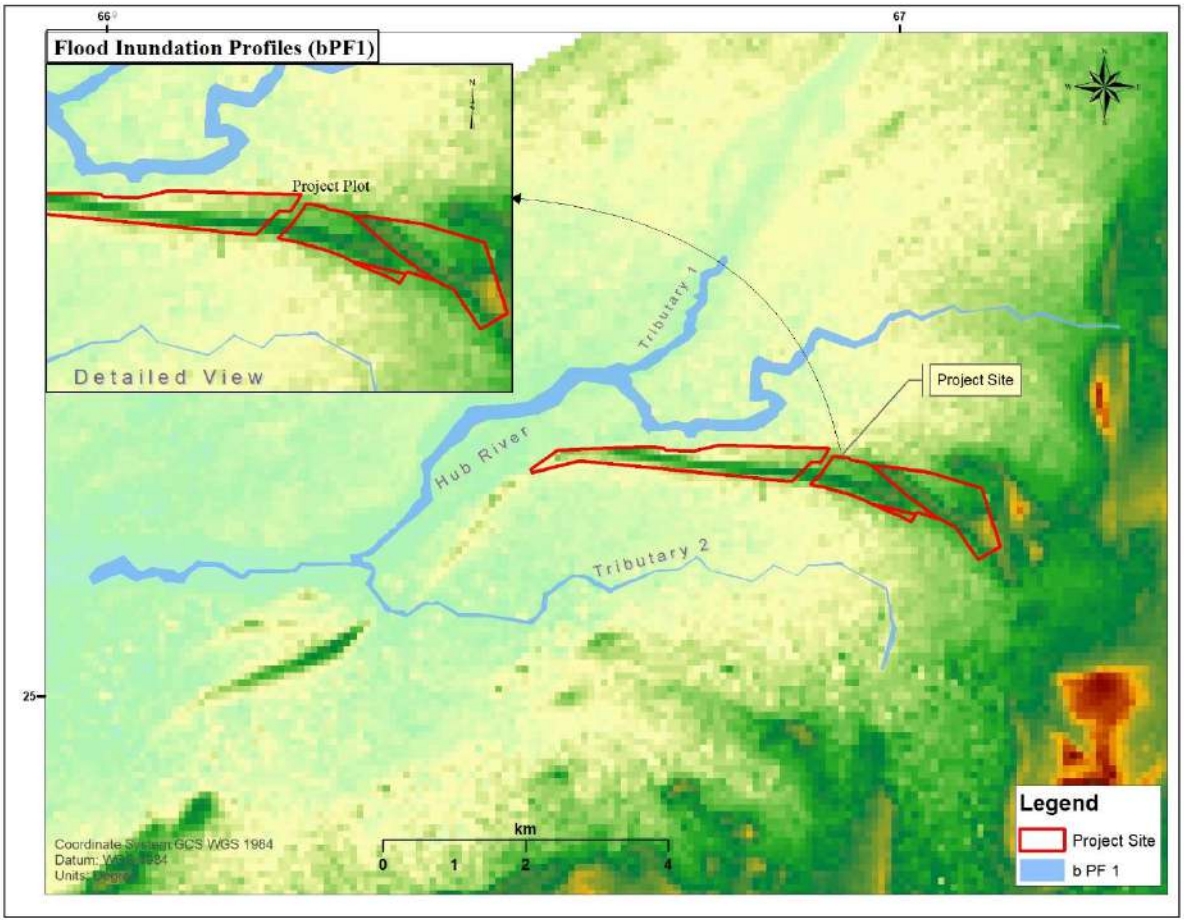

Figure 7-14: HEC-RAS model discharge profile b PF 1

7.6.4 Flood Inundation Proile (s PF 1)

The HEC-RAS model generates a base flow (s PF 1) of the stream, as shown in the (Figure 7-15)**.** The maximum flow of the stream during peak flood inundates the existing banks of the stream. The (s PF 1) includes calculations for the stress flow of the stream.

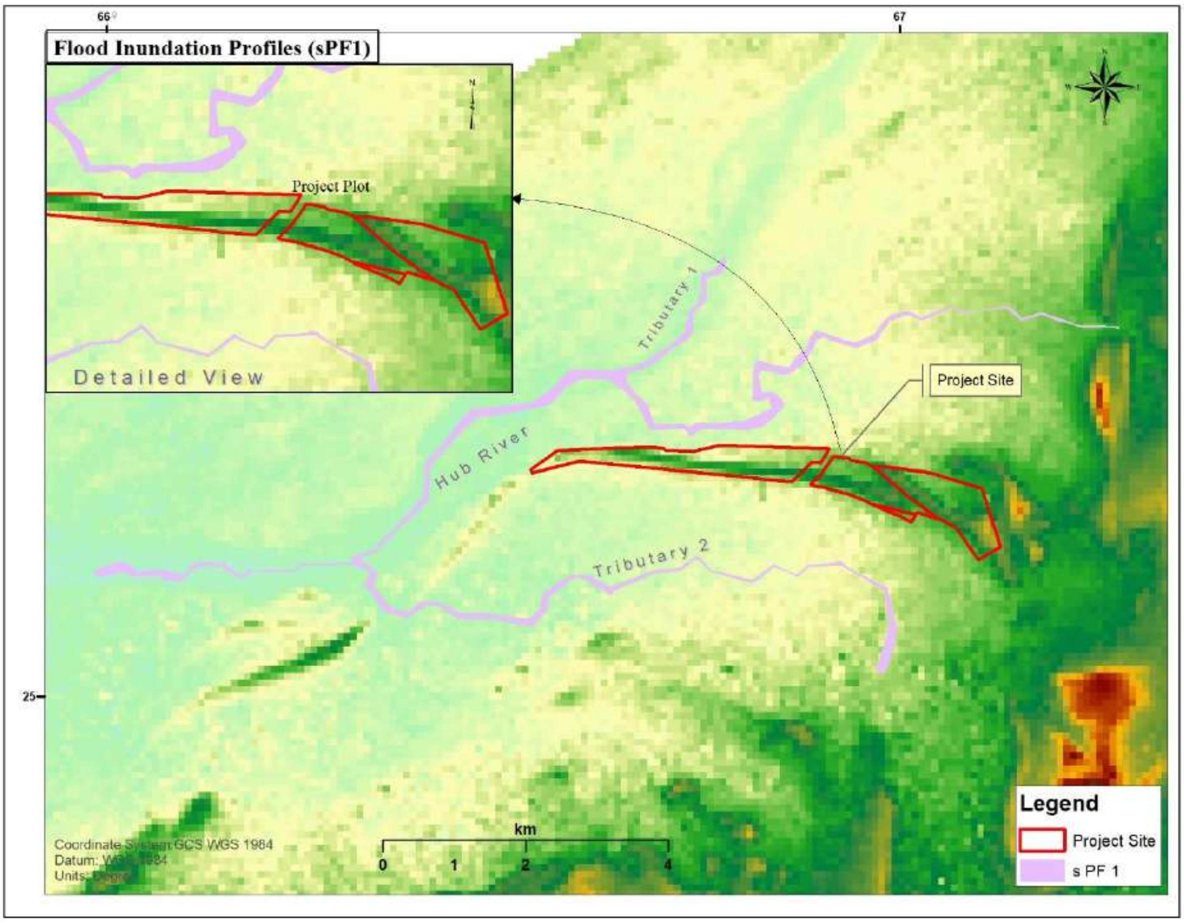

Figure 7-15: HEC-RAS model discharge profile s PF 1

7.6.5 Flood Inundation Proile (d PF 1)

On the basis of HEC-RAS model final outputs generate a deposition (d PF 1) profile in ArcGIS environment, the deposition profile of the stream along its banks, as shown in (**Figure 7-16)**. The parameters used to define the deposition along the banks include resistance factors such as the existing stream bed conditions, slopes, elevation, land use, and land cover of the stream area. These depositions are determined based on the conditions provided in the model simulations. The maximum flow of the stream during peak flood inundates the existing banks of the stream and generates a deposition profile. The (d PF 1) profile illustrates the extent of maximum deposition during flood events, as shown in (**Figure 7-16).**

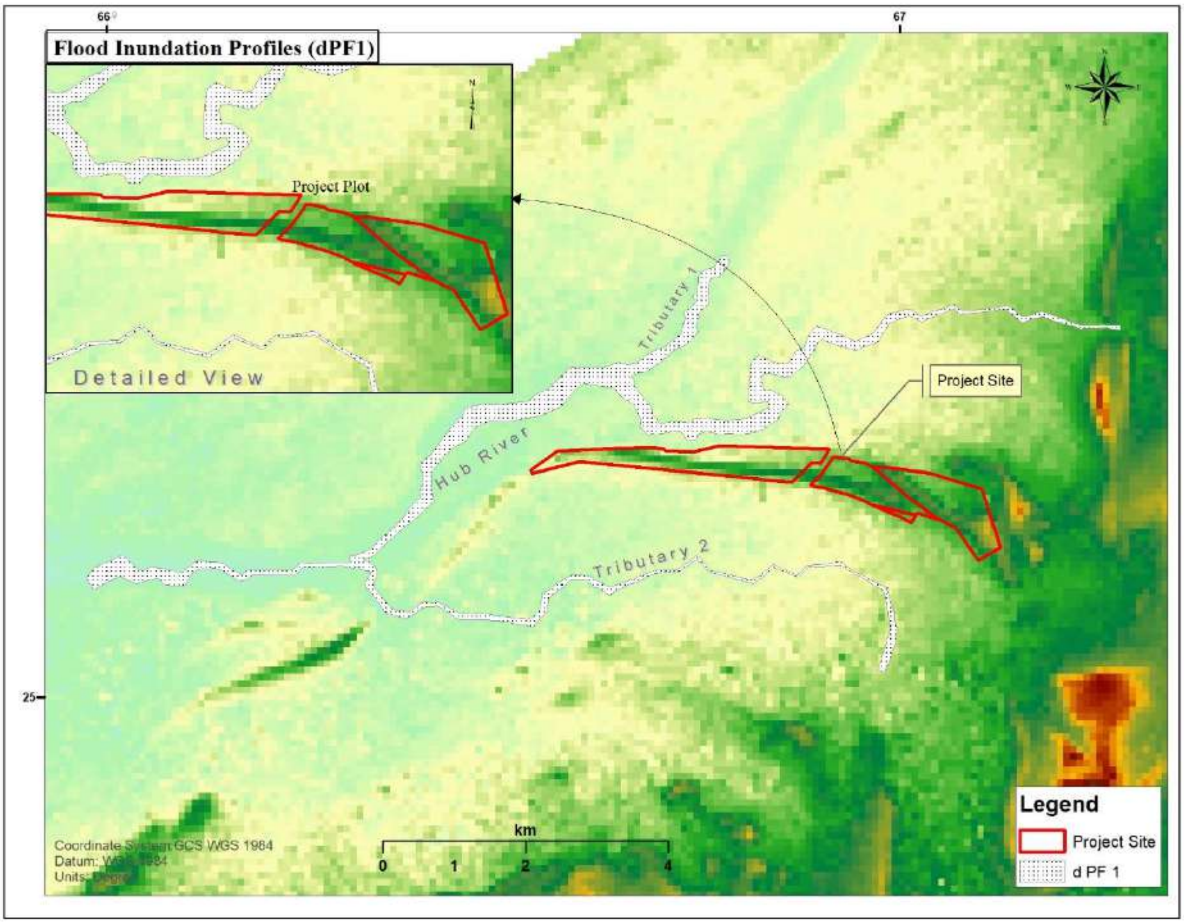

Figure 7-16: HEC-RAS model deposition profile d PF 1

7.7 Flood Inundation Proiles (v PF 1, s PF 1, b PF 1 and d PF 1)

The numbers of the calculated profiles were determined based on the study objectives, on the basis of HEC-RAS model final outputs generate a multiple flood inundation profiles against discharge of the stream in ArcGIS environment. The cumulative discharges of the stream present in (**Table 8-1**). The profile generated on base of peak flood include (v PF 1, s PF 1, b PF 1 and d PF 1) which is shown in (**Figure 7-16**). The parameters used to calculate the flood inundation area along the banks include stream flow resistance factors such as the existing stream bed profiling, slopes, elevation, land use, and land cover of the stream area. These flood inundation profiles are determined based on the conditions provided to the model simulations. The maximum flow of the stream during peak flood inundates the existing banks of the stream and generates a multiple profile which is shown in (**Figure 7-16).**

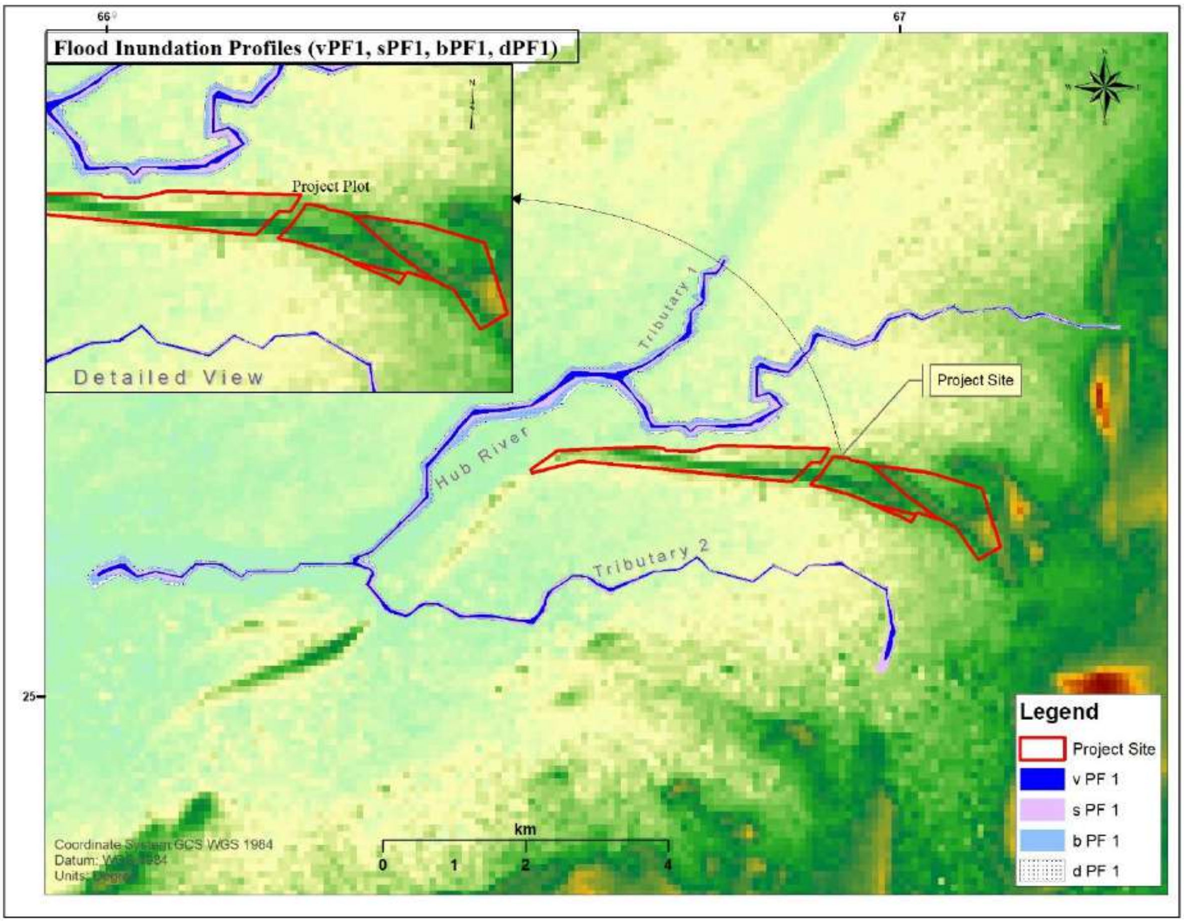

Figure 7-17: HEC-RAS model flood inundation profiles

7.7.1 Assessments based on flood inundation profiles

The Flood Analysis Model is based on extensive precipitation data collected by NASA Power and SolarGIS. The report presents flood levels at different elevation levels, including peak flood extent profiles of nearby streams. During heavy rainfall seasons, the main flood hotspots are identified and modeled. Although the likelihood of flooding in the region is low, a ground topographic survey has determined that the minimum elevation for flood inundation is 57 meters. The upper reach of the project area is less vulnerable to flooding, while the lower reach with its low slopes and uneven terrain is more susceptible to flash floods during heavy rainfall seasons. To address this issue, civil infrastructure may need to be implemented to prevent water stagnation in certain areas. Overall, the flood risk to the project is considered to be very low, as per the (Flood Inundation) analysis.

Flood analysis was carried out for short-term and long-term rainstorms by using their respective total and excess hyetographs. To simulate flood events from the selected rainstorms, soil map, land use map and DEM with 12.5 m pixel resolution was used as the model input data layers. A special emphasis was given to defining the extent and magnitude of flooding within the boundary condition during events in the plot site. The defined boundary conditions allowed to determine the extent, depth, and behavior of flood flows within the plot area. Before reviewing the model results, it is highly possible to presume no flooding risk the designed project module's locations based on field assessments. The patches proposed to install PV shed is safe in terms of flood and active run over or water accumulation when heavy rains occur. No active ravine erosion is observed around PV shed location and its potential is very low, accommodating there is no landslide indication is observed. Before project construction the land leveling is also recommended in result the heavy rain water can easily flow at project site lower reaches. It is analyzed that there is low probability to impact small parcel of project land in case of heavy rainfall events which is not a major impact on project capacity.

The impact of the heavy meteorological events is inversely influence on the land use, landcover and topography of the project land and its watershed, however the Pakistan is prone to climate change therefore the weather pattern shifts may directly or indirectly impact on the meteorological parameters at country level. In result a specific percentage are added in metrological parameters on basis of climate change predicting factor [5].

8 HYDROLOGY AND DISCHARGE ANALYSIS OF THE STREAMS

8.1 Discharges of the streams Long-term (1999-2022)

The data for the stream flow covers the period from (1999 – 2022). It can be observed that the discharge of the streams has increased over the last decade. The highest peak discharge of the river was recorded from June to August in 2022. (**Table 8-1**) present the total discharge of the neighboring streams at the outlet of the project site.

Table 8-1: Anual and monthly discharges of the stream

	Jan	Feb	Mar	Apr	May	Jun	Jul	Aug	Sep	Oct	Nov	Dec	Year	
1999	71.52	8.86	93.07	139.10	208.15	415.29	479.48	419.29	187.13	119.37	98.48	75.05	2398.79	1999
2000	62.89	72.72	80.80	121.20	181.80	330.55	415.55	363.61	161.60	103.89	85.56	63.24	2043.42	2000
2001	147.04	171.59	190.66	285.99	428.99	779.97	980.54	857.97	381.32	245.13	201.88	149.21	4819.29	2001
2002	51.64	59.50	66.11	99.17	148.75	270.45	340.00	297.50	132.22	85.00	70.00	51.74	1671.07	2002
2003	289.45	338.93	376.59	564.88	847.32	1540.58	1936.73	1694.64	753.17	484.18	399.74	294.72	9518.93	2003
2004	77.52	89.91	99.90	149.85	224.78	408.68	513.78	449.55	199.80	128.44	105.78	78.18	2525.18	2004
2005	78.65	91.23	101.37	153.05	228.08	414.69	521.33	456.16	202.74	130.33	107.33	79.33	2562.31	2005
2006	319.83	374.63	416.25	624.38	936.57	1702.85	2140.73	1873.14	832.51	535.18	440.74	325.76	10521.57	2006
2007	299.45	350.68	389.65	584.47	876.70	1594.00	2003.89	1753.40	779.29	500.97	412.57	304.94	9849.02	2007
2008	132.91	154.99	172.21	258.32	387.48	704.51	885.67	774.97	344.43	221.42	182.34	134.78	4353.04	2008
2009	163.29	190.69	211.88	317.82	479.73	866.79	1089.67	953.46	423.76	272.42	224.34	165.82	5355.69	2009
2010	342.21	400.93	445.47	668.21	1002.31	1822.39	2291.00	2004.63	890.94	572.75	471.68	348.63	11260.15	2010
2011	371.35	435.16	483.51	725.26	1087.89	1977.98	2486.60	2175.78	967.01	621.65	511.95	378.40	12228.53	2011
2012	87.40	101.52	112.80	169.19	253.79	461.44	580.10	507.58	225.59	145.02	119.43	88.28	2857.14	2012
2013	185.30	216.55	240.61	360.92	541.37	984.32	1237.43	1082.75	481.22	309.36	254.76	188.30	6087.88	2013
2014	94.65	110.04	122.26	183.40	275.09	500.17	628.79	550.19	244.53	157.20	129.46	95.68	3090.45	2014
2015	84.65	98.28	109.21	163.81	245.71	446.75	561.63	491.42	218.41	140.41	115.63	85.46	2764.37	2015
2016	138.29	161.31	179.23	268.85	403.28	735.23	921.77	806.55	358.47	230.44	189.78	140.27	4534.47	2016
2017	217.81	254.75	283.05	424.58	636.87	1157.94	1455.70	1273.73	566.10	363.92	299.70	221.52	7157.67	2017
2018	45.01	51.71	57.46	86.19	129.28	235.06	295.50	258.57	114.92	73.88	60.84	44.97	1454.39	2018
2019	413.86	485.11	539.01	808.51	1212.77	2205.03	2772.04	2425.53	1078.01	693.01	570.71	421.83	13629.41	2019
2020	200.68	234.62	260.69	391.03	586.55	1066.45	1340.68	1173.10	521.38	335.17	276.02	204.02	6590.39	2020
2021	168.04	190.40	211.55	317.33	476.00	865.45	1087.99	952.00	423.11	272.00	224.00	165.56	5349.44	2021
2022	649.29	760.57	845.08	1267.61	1901.42	3457.13	4346.10	3802.84	1690.15	1086.53	894.79	661.36	21690.86	2022
LTA	205.73	238.20	267.67	397.01	596.51	1087.38	1361.16	1195.02	531.34	343.29	282.24	209.13	6791.67	LTA

Long-term statistics is calculated from complete years

Yearly sum (cfs)

8.2 Flood Hydrographs

The morphological changes in a riverbed can be exacerbated by the impacts of climate change, particularly through the heightened frequency of extreme climatic events such as floods. To assess these changes, flood volumes and durations were determined by extracting the baseflow from measured discharge data and fitting suitable marginal distribution functions to the peak discharge (Q), flood volume (V), and duration (D) data. The physical factors that impact flood hydrodynamics include the shape of the drainage basin, topography and relief, intense storms, prolonged rainfall, snowfall, vegetation, and rock type. The **(Figure** 8-1**)** below depicts the flood hydrodynamics of the project site, based on long-term calculated discharges of the stream. The baseflow of the river is shown in the **(Figure** 8-1**)**, representing the flow that reaches the channel through slow through flow and permeable rock below the water table. As stormwater enters the drainage basin, the discharge rates increase, as illustrated by the hydrograph calculated for the river basin and each individual recorded storm event, demonstrating how different levels of precipitation impact a river during a storm.

The rate at which the hydrograph rises and falls is based on the Tc and a rise/fall factor. For "standard" Rational method, the rise and fall factors are both one. That is, the rise and fall occur over the exact interval Tc. Variations of the Rational method (often called the Modified Rational method), may use different rise and fall factors [2].

$$Q_p = CiA$$

$$i = \frac{precipitation\left(\frac{mm}{annum}\right)}{Time(annual)}$$

$$V = A \times i$$

where
Q_p= Peak Discharge (cubic feet/sec)
C=Runoff coefficient
i= Intensity (inch/hour)
V= Volume (cubic feet/sec)
A= Area (acres)

The Rainfall intensity $'i'$ is typically found from Intensity/Duration/Frequency curves for rainfall events in the geographical region of interest. The duration is usually equivalent to the time of concentration of the drainage area. The storm frequency is typically stated by local authorities depending on the impact of the development. A 10-yr, 25-yr, 50-yr, or even 100-yr storm frequency may be specified.

The peak discharges of the streams were calculated over a period from (1999 to 2022), revealing an increase in the flow of the channel over time (**Table 8-1)**. The initial peak discharge was calculated to be Q_1 1787.18 cubic feet per second (cfs) at the start of the year 1999, whereas the discharge calculated over the selected period was Q_2 9019.45 cfs. The maximum peak discharge recorded 7during the last 23 years occurred in July 2022, with a value of Q_3 17235.86 cfs. The peak discharges and baseflow of the stream have been calculated and are displayed in (**Table 8-3**).

Baseflow

The baseflow for the period between 1999 and 2022 was determined by computing the cumulative stream flows. The baseflow over the last 23 years was calculated. The estimated baseflows are presented in (**Table 8-3**) and illustrated in below (**Figure** 8-1**).**

$$Base\ flow = Peak\ Discharge - Constant\ (85)$$

where
Base flow =$cubic\ feet\ per\ second\ (cfs)$
Peak Discharge = $cubic\ feet\ per\ second\ (cfs)$

Runoff hydrograph

A runoff hydrograph reflects the accumulated runoff from both surface and subsurface (base flow) runoff. The surface runoff or direct runoff hydrograph is derived from the overall storm hydrograph by separating the base flow component. This hydrograph is depicted in (**Figure** 8-1**).**

$$Runoff\ hydrograph = \frac{Volume}{Area}$$

where
Volume = ft^3/sec
Area = $acres$

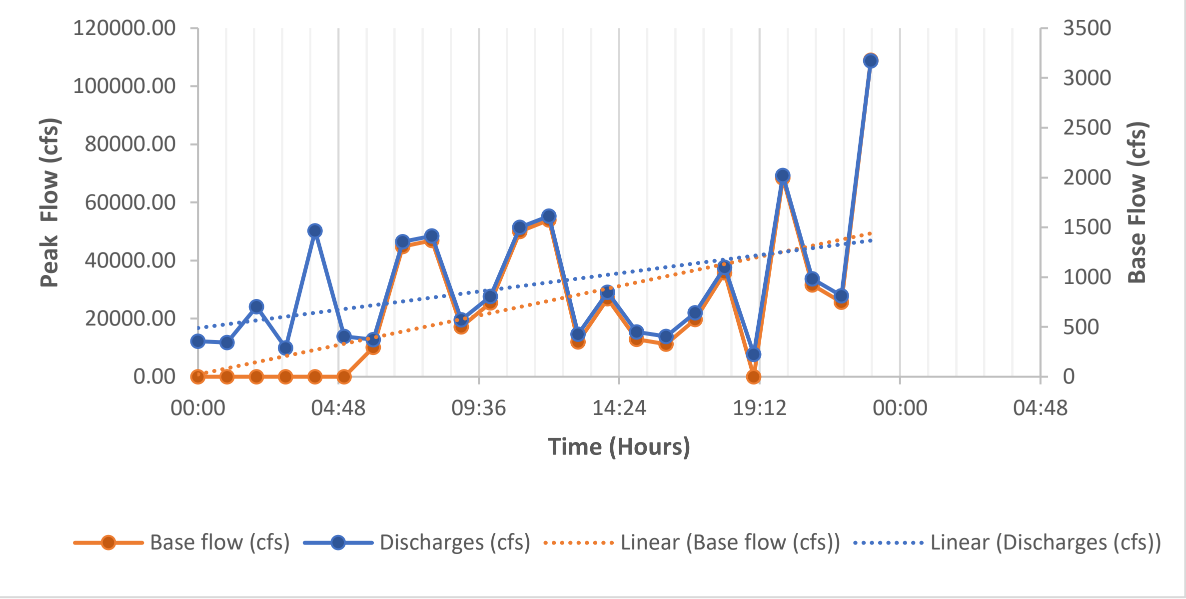

Figure 8-1: Flood hydrograph

8.3 Return period (Probability of occurrence)

The return period of the flood was determined by sorting the stream's flow data from maximum to minimum, and calculating the probability of exceeding a specified flow. A plot of flood magnitude against return time was generated. The formula utilized for calculating the Return Period (RP) and Probability of Exceedance (PO) values is:

$$Probability\ of\ occurrence\ (fa\%) = \frac{100(2n-1)}{2y}$$

$$Return\ period = \frac{100}{\%age\ of\ probability\ of\ occurrence}$$

where
Rank of each events = "n"
Total number of events = "y"
Percentage Probability of occurrence = %fa

The calculated values compared to the flow data are displayed in (**Figure 8-2), (Table 8-2).**

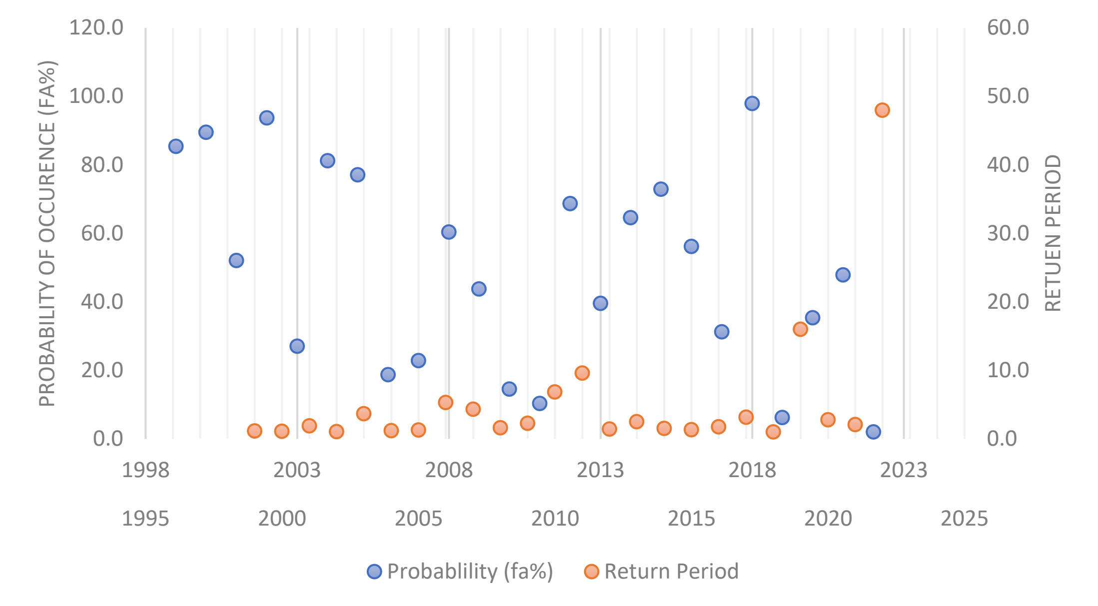

Figure 8-2: Return period and probability of exceedance at the given period.

Table 8-2: Return period calculated values

Annual Precipitation for project area							
Years	Depth (mm)	Rank	Years	Depth (mm)	Rank	Probability (fa%)	Return Period
1999	57.4	1	2022	518.7	1	2.1	49.0
2000	49.9	2	2019	332.2	2	6.3	17.0
2001	117.8	3	2011	298.2	3	10.4	9.6
2002	41.5	4	2010	275.9	4	14.6	6.9
2003	233.7	5	2006	258	5	18.8	6.3
2004	62.2	6	2007	239.7	6	22.9	4.4
2005	64.1	7	2003	240.7	7	27.1	3.7
2006	257	8	2017	175.4	8	31.3	3.2
2007	239.7	9	2020	159.9	9	35.4	2.9
2008	106.5	10	2013	147.4	10	39.6	2.5
2009	139.8	11	2009	129.9	11	43.8	2.3
2010	273.9	12	2021	129.6	12	47.9	2.5
2011	297.2	13	2001	117.8	13	52.1	1.9
2012	69.8	14	2016	109.8	14	56.3	1.9
2013	157.4	15	2008	105.5	15	60.4	1.8
2014	75.9	16	2014	74.9	16	64.6	1.6
2015	67.9	17	2012	69.1	17	68.8	1.6
2016	109.9	18	2015	66.9	18	72.9	1.5
2017	183.4	19	2005	62.1	19	77.1	1.4
2018	36.2	20	2004	61.2	20	81.3	1.3
2019	340.2	21	1999	56.4	21	85.4	1.3
2020	169.7	22	2000	49.5	22	89.6	1.2
2021	139.6	23	2002	40.5	23	93.8	1.2
2022	527.7	24	2018	35.2	24	97.9	1.0

8.4 Frequency of the flood discharges

The frequency of the hydrograph over the period 1999-2022, which reflects the difference between the peak discharges and the baseflow of the stream, has been calculated. The resulting frequency is depicted in (**Figure 8-3)**, and the estimated values are presented in (**Table 8-3**). The formula utilized to calculate frequency is:

$$Frequency = Peak\ Discharge - Base\ flow$$

where
Peak Discharge = ft^3/sec
Base Flow = ft^3/sec

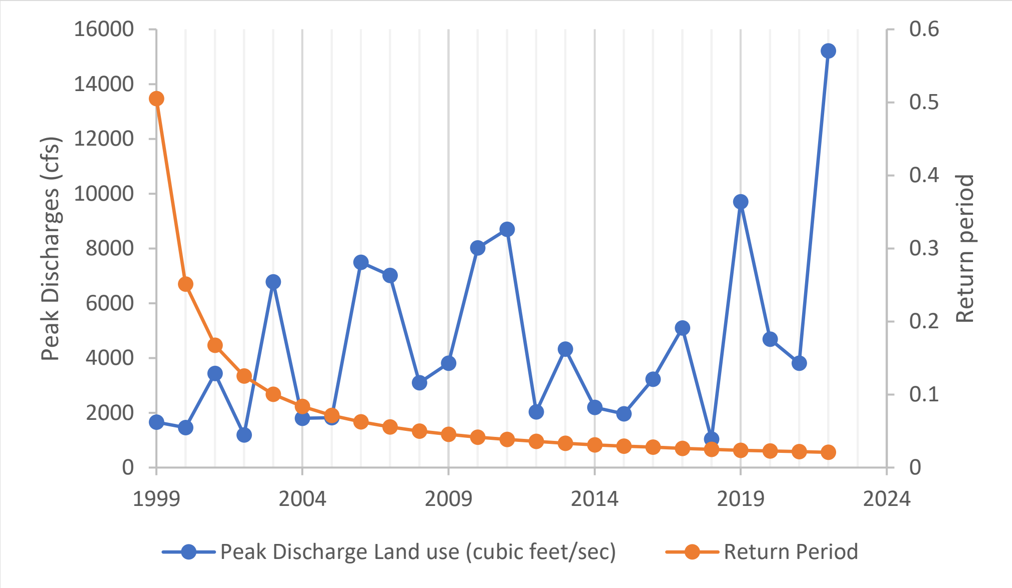

Figure 8-3: Frequency distribution of the estimated flood (1999-2022)

Table 8-3: Flood frequencey and estimated discharges

Years	Time Period (hrs)	Discharges (cfs)	Base Flow (cfs)	Frequency
1999	0:00	1667.18	0.00	1658.18
2000	1:00	1464.44	0.00	1455.44
2001	2:00	3441.88	0.00	3432.88
2002	3:00	1199.99	0.00	1189.99
2003	4:00	6779.56	0.00	6779.56
2004	5:00	1799.21	0.00	1799.21
2005	6:00	1825.66	0.00	1825.66
2006	7:00	7494.56	261599.58	85.00
2007	8:00	7014.62	244685.11	85.00
2008	9:00	3099.99	106469.91	85.00
2009	10:00	3814.86	131685.48	85.00
2010	11:00	8019.50	280179.28	85.00
2011	12:00	8704.12	304346.21	85.00
2012	13:00	2030.85	68699.94	85.00
2013	14:00	4331.99	149945.89	85.00
2014	15:00	2200.98	74718.23	85.00
2015	16:00	1966.69	66417.14	85.00
2016	17:00	3227.21	110930.75	85.00
2017	18:00	5095.94	176924.44	85.00
2018	19:00	1035.27	33523.06	85.00
2019	20:00	9703.12	339626.86	85.00
2020	21:00	4693.40	162708.82	85.00
2021	22:00	3808.98	131475.95	85.00
2022	23:00	15212.36	534183.72	85.00

8.5 Long-term probability of flood occurrence graph

The flood discharges of Deh Halkani and its surrounding streams have been estimated using a model designed to evaluate the extent of flood inundation. The impact of the calculated flow data on the Solar PV project site has been assessed. Linear regression analysis was utilized to make a long-term flood forecast based on the modeled historical flood events. The forecasted flood graph shown in below (**Figure 8-4).**

$$Y_i = f(X_i, \beta) + e_i$$

where
Dependent variable = Y_i
Function = f
Independent variable = X_i
Unknown Parameter = β
Error Terms = e_i

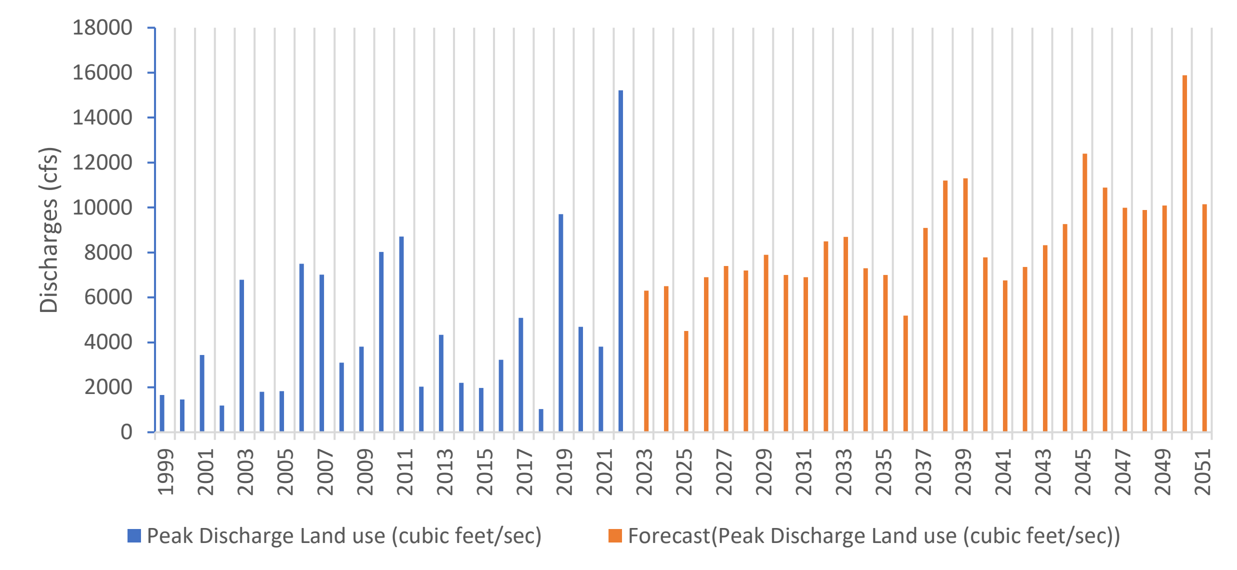

Figure 8-4: Long-term flood forecasted (1999-2051)

8.6 Time of Concentration

The time of concentration is a crucial watershed parameter that is used to calculate the peak discharge of a watershed. This peak discharge is dependent on the rainfall intensity, which is based on the time of concentration. The time of concentration represents the maximum time required for a particle to travel from the watershed divide to the watershed outlet. It is a concept employed in hydrology to gauge the response of a watershed to a rain event and is determined by the watershed's topography, geology, and land use.

The parameters used in the calculation include catchment area, runoff coefficient, and time of concentration [6]. The time of concentration was obtained using the Kirpich method with the following formula:

$$t_c = 0.0195 \left({}^{L}/_{\sqrt{S}} \right)^{0.77}$$

where

t_c= Time Concentration (minutes)
L= Channel Flow Length (meters)
S= Dimensionless Main Channel Slope

Time of concentration for all the three watershed tributaries are present in (**Table 8-4**).

Table 8-4: Time of Concentration of the main chanel and tributaries

Water Sheds	Area of sub-basin (Acres)	Length of Tributaries (m)	Rainfall mm/annum	Slope (%)	Estimated discharges (cfs)	Time Concentration (Min)
1	4703	31560	517.9	32.04	871.8	14.09
2	299840	33898	517.9	20.6	5806.63	18.16
3	467593	85489	517.9	24	8967.86	33.45

The estimated concentration time for the runoff water to reach its outlet-1 after precipitation is approximately 14.09 minutes. At the watershed, the estimated time for the water to reach its outlet-2 is around 18.16 minutes. However, at watershed three, the estimated time for the water to reach its outlet-3 is approximately 33.45 minutes. The catchment area for these water channels is illustrated in **(Figure 7-3).**

9 PV Solar Structure and Rain Water Drainage within project plot

The Halkani PV Solar Site has a total project area of approximately 612 acres. There are two distinct photovoltaic (PV) solar installation scenarios: one is a fixed tilt installation with a capacity of 200 MW, and the other is a single axis installation with a capacity of 120 MW. The single axis installation encompasses nearly the entire project area, which is approximately 612 acres. The assessment of natural rainwater flow within the project plot was based on a ground topographic survey and terrain analysis.

The project land features a merged terrain, with multiple small catchments within its borders. Despite rainstorms, rainwater does not accumulate on the land due to its terrain nature. The land is divided into three different nature slopes, owing to the existence of a small hilltop in the project land area. However, the natural flow of rainwater is not unidirectional within the project land. The upper portion of the land and its slopes face northwest, and the lower part of the project land slope faces towards the south. Meanwhile, the west side of the land slopes faces west. Due to the different facing of slopes, the rainwater is not combined in a single outlet. As a result, there is a low chance of rainwater accumulation even during heavy rainstorms. However, it is recommended that land leveling be performed during the construction phase of the PV structure installation site, and that the rainwater flow be sloped as per the natural flow of the land.

9.1 PV solar site and Elevations profiles

The PV project site is shown in **(**Figure 9-1**)** based on the elevation profile. The natural flow of rainwater channels during rainy seasons was captured using data from a ground topographic survey. The PV solar plant design were based on the contour map of the project plot. The proposed drainage ditches and structures are described in a subsequent section of the report.

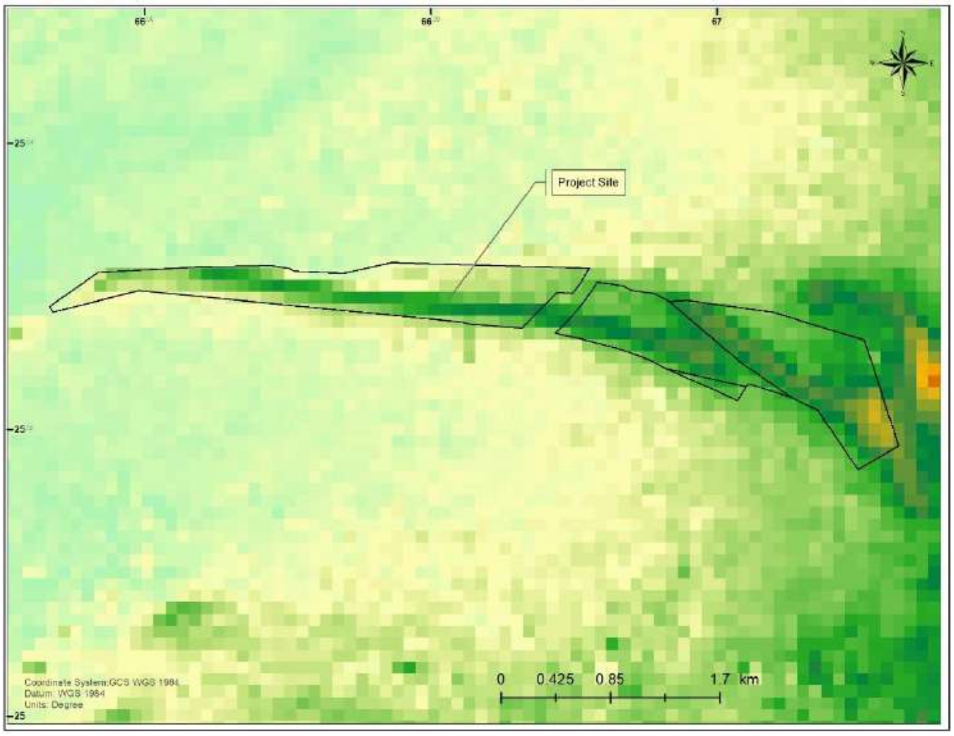

Figure 9-1: Project site and elevation profile

The culverts and drainage ditches proposed within the project plot have been designed to conform to the natural flow and terrain of the region. During heavy rainfall seasons, there is a likelihood that the flow of perennial channels may impact the PV solar structures. The location coordinates for each drainage ditch and culvert are detailed in a later section of the report.

9.2 PV solar structures and drainage system within project plot

The project plot is home to multiple small rainwater channels, or "Nullahs", which have small catchment areas and the potential to carry flowing water during heavy rainfall. The design of the proposed photovoltaic (PV) solar structure and rainwater drainage ditches is based on the natural flow of water and the results of a ground-based topographic survey. During the site survey, multiple small rainwater channels were identified within the project plot, including one on the northeast of the site. The maximum project catchment is located under this northeast Nullah, and the natural flow of rainwater is from the northeast to the south. The lowest elevation at the outlet at the project boundary is approximately 56m. A permanent drainage ditches has been proposed to manage the flow of rainwater, as shown in **(Figure 9-2).** The coordinates of the proposed drainage ditches are listed in table below:

Rainwater Drainage - 2		
S. No	**Latitude**	**Longitude**
1	25° 1'50.75"N	66°59'58.12"E
2	25° 1'53.32"N	66°59'54.14"E
3	25° 1'54.36"N	66°59'50.49"E
4	25° 1'55.00"N	66°59'47.61"E

5	25° 1'58.36"N	66°59'45.37"E
6	25° 2'0.85"N	66°59'42.90"E
7	25° 1'48.76"N	66°59'45.08"E
8	25° 1'56.34"N	66°59'43.20"E

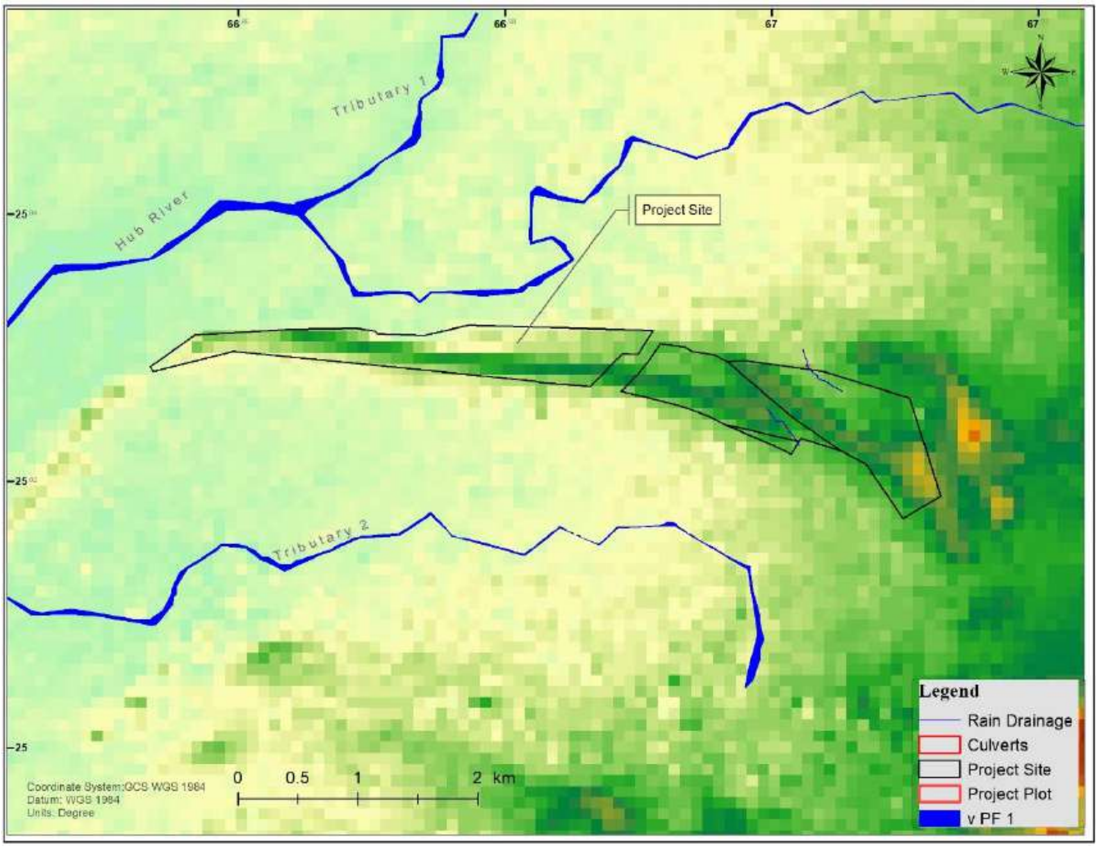

Figure 9-2: Rainwater drainage structures and terrain

The proposed drainage ditches and culverts for managing rainwater are depicted in the above **(Figure 9-2).** The culverts have been proposed at various locations based on the existing terrain, flow of rainwater and topographic profile. The middle part of the project area features high slopes and includes a small hill where it is not feasible to install the PV solar structure. Ground clearance and land leveling are necessary during the construction phase.

Table 9-1: Proposed culvert loction within project plot

Culverts Locations (DMS)		
S. No	Latitude	Longitude
1	25° 1'55.46"N	66°58'50.73"E
2	25° 1'53.35"N	66°59'22.76"E
3	25° 1'24.50"N	66°59'33.92"E

Rainwater Drainage - 2		
S. No	Latitude	Longitude
1	25° 1'50.75"N	66°59'58.12"E
2	25° 1'53.32"N	66°59'54.14"E
3	25° 1'54.36"N	66°59'50.49"E
4	25° 1'55.00"N	66°59'47.61"E
5	25° 1'58.36"N	66°59'45.37"E
6	25° 2'0.85"N	66°59'42.90"E

7	25° 1'48.76"N	66°59'45.08"E
8	25° 1'56.34"N	66°59'43.20"E

Table 9-2: Proposed rainwater drainage channels Locations

Rainwater Drainage – 1 (DMS)		
S. No	**Latitude**	**Longitude**
1	25° 1'57.62"N	66°58'29.03"E
2	25° 1'58.41"N	66°58'35.53"E
3	25° 1'55.93"N	66°58'37.80"E
4	25° 1'55.75"N	66°58'45.26"E
5	25° 1'55.61"N	66°58'50.70"E
6	25° 1'53.25"N	66°59'10.80"E
7	25° 1'53.44"N	66°59'21.48"E
8	25° 1'51.62"N	66°59'27.84"E

10 CONCLUSIONS AND WAY FORWARDS

The HUB River basin, which is the largest and closest water basin to the plot site, has its main riverbed located 30 meters lower and 1.8 kilometers away from the plot site. Despite the scale and duration of potential floods, the designed solar PV structures are not vulnerable to any flood risk. A significant part of the plot area lies within the right tributary basin, where short-term floods occur during rainstorms. However, the solar PV locations have been strategically placed at an elevation 40 meters higher than the riverbed and floodplain, eliminating the risk of floods from the HUB river. The HUB River, another perennial tributary situated 1.65 kilometers away from the plot site, is also not considered a potential threat to the solar PV farm area.

- The proposed land use is planned according to the site's drainage pattern, with development near streams and steep slopes to be avoided.
- Detailed engineering and design should reference the maximum levels of flood flow.
- The site is safe from flood and active run-over or water accumulation during heavy rain events.
- No active ravine erosion has been observed around the project installation solar PV structures, and its potential is considered very low.
- Adequate drainage facilities and flood water channels must be provided to handle flow during flood events to ensure structural stability and safety.
- The project site is part of a normal watershed, receiving surface runoff from the catchment area with a normal flush flow.
- Based on above ground observations, it is recommended that engineering structures like causeways or anchored RCC pavements be provided over stream crossings to mitigate flood-associated risks.
- Streams with parallel flow in the project area will be controlled by raising the finished road level with sufficient side protection.

- Scattered flow will be managed by providing side trenches and protection embankments which are proposed in report section-9
- Based on the above comments, a mitigation plan for the project area should be developed, and the description of proposed hydrological measures finalized by the developer.
- Overall, the flood risk to the project is considered very low as per the Flood Inundation analysis.

11 REFERENCES

[1] US Army Corps of Engineers-Hydrologic Engineering Center, 2009, HEC GeoRAS User's Manual version 4.2.93, HEC-GeoRAS: GIS tools for Support of HEC-RAS using ArcGIS http://www.hec.usace.army.mil/softwarelhec

[2] Yang, J., Townsend, R.D. and Daneshfar, B., 2006. Applying the HEC-RAS model and GIS techniques in river network floodplain delineation. Canadian Journal of Civil Engineering, 33(1), pp.19-28.

[3] Weikel, J., Karki, R. and Cibin, R., 2022. Evaluating the Hydrologic and Water Quality Impacts of the Revised SCS CN Method and its Implications on Decision-making. Journal of the ASABE, 65(6), pp.1451-1464.

[4] Khattak, M.S., Anwar, F., Saeed, T.U., Sharif, M., Sheraz, K. and Ahmed, A., 2016. Floodplain mapping using HEC-RAS and ArcGIS: a case study of Kabul River. Arabian Journal for Science and Engineering, 41, pp.1375-1390.

[5] DEFRA,(2006) "The UK Flood and Coastal Defence Appraisal Guidance FCDPAG3 Economic Appraisal – Supplementary note to Operating Authorities – Climate Change Impacts, OCT 2006.

[6] Telemac(2014) "TELEMAC-2D Modelling Software System for 2-D hydrodynamics", Release 7.2User Manual December 2017

12 APPENDIX

Annex A Temperature and Rainfall Maps of Pakistan[5], [6]

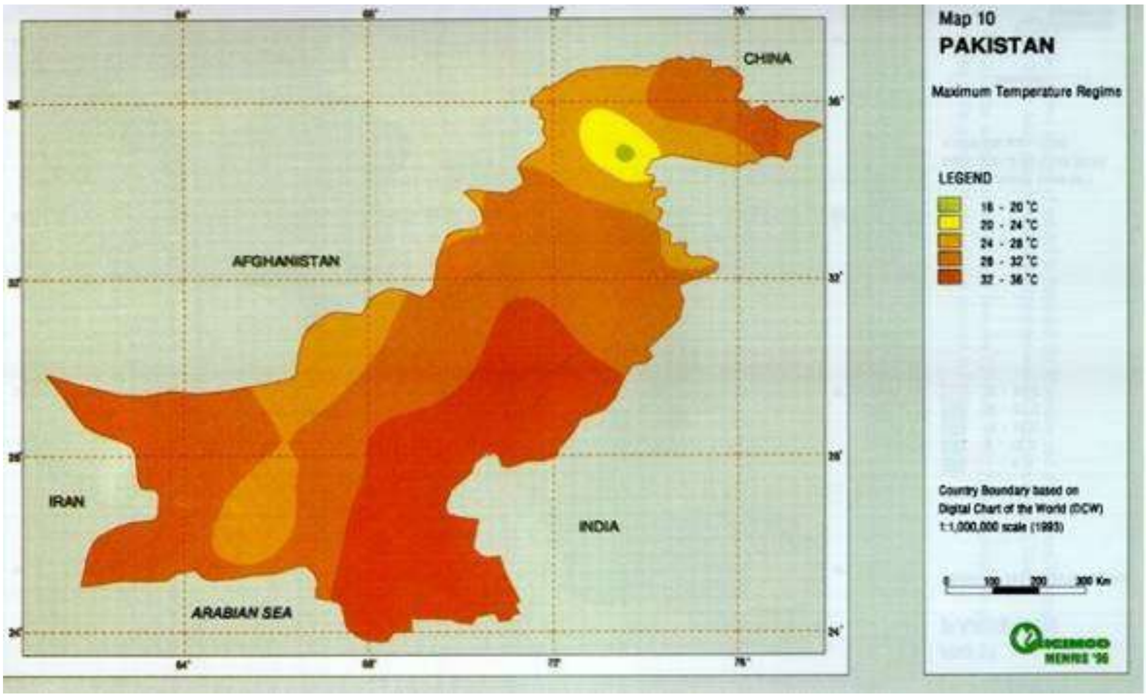

Maximum Temperature Regime Map of Pakistan

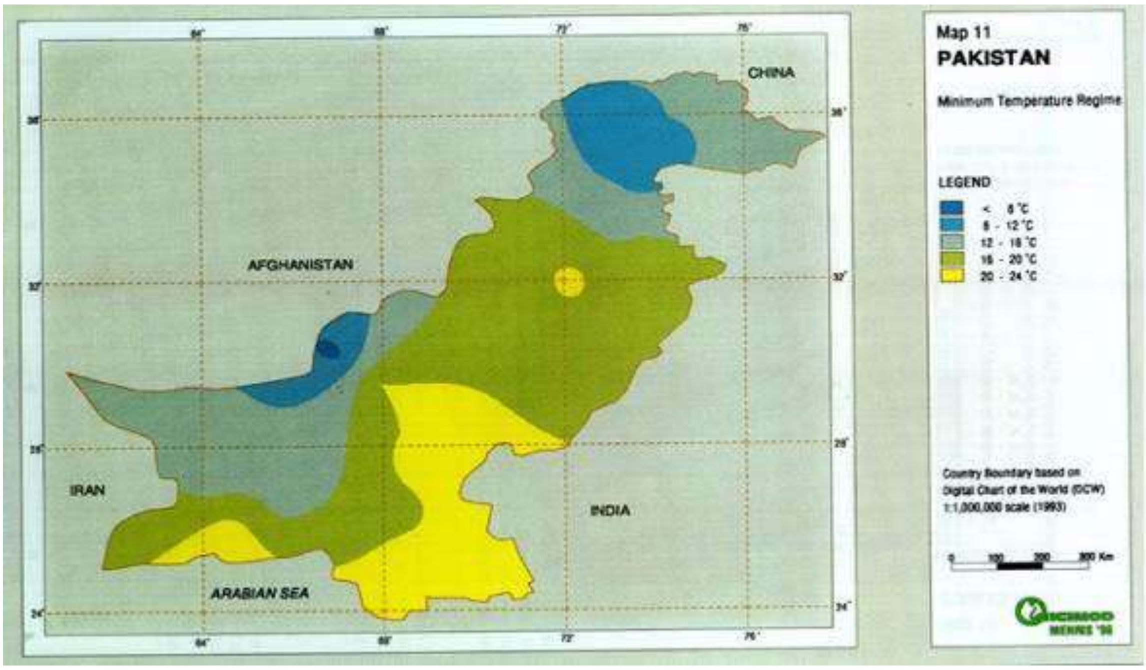

Minimum Temperature Regime Map of Pakistan

---

[5] Survey of Pakistan

[6] Pakistan Meteorological Department (PMD)

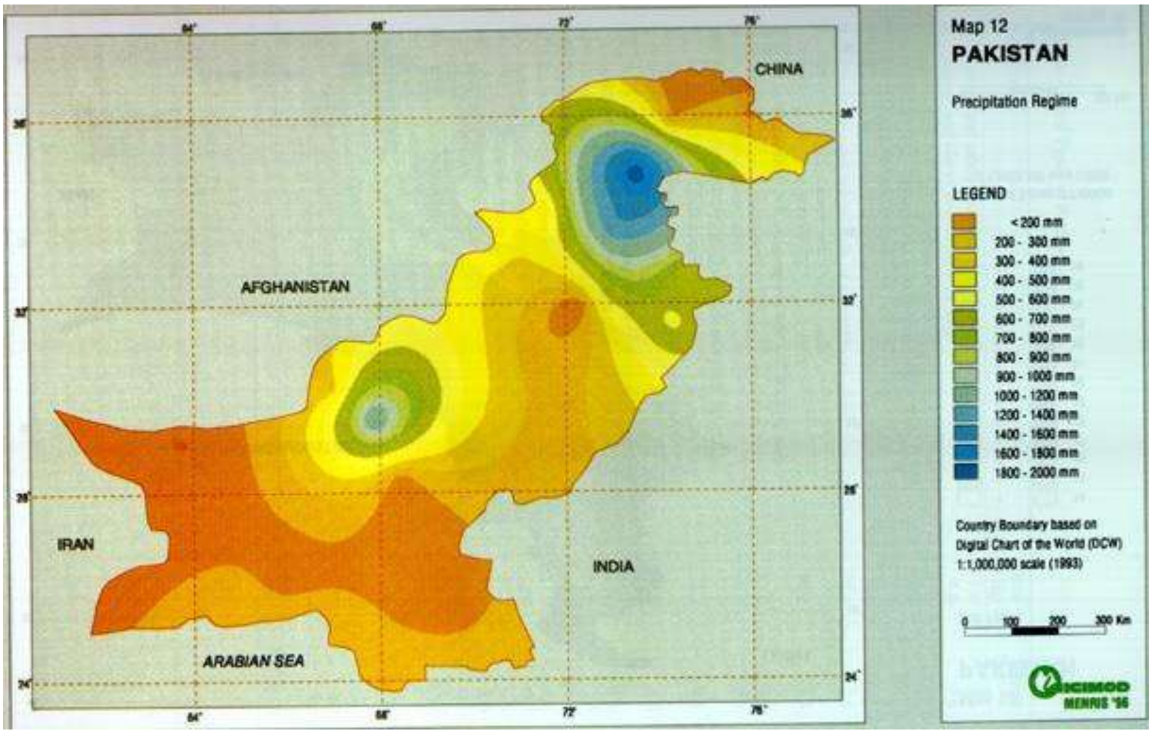

Rainfall Map of Pakistan

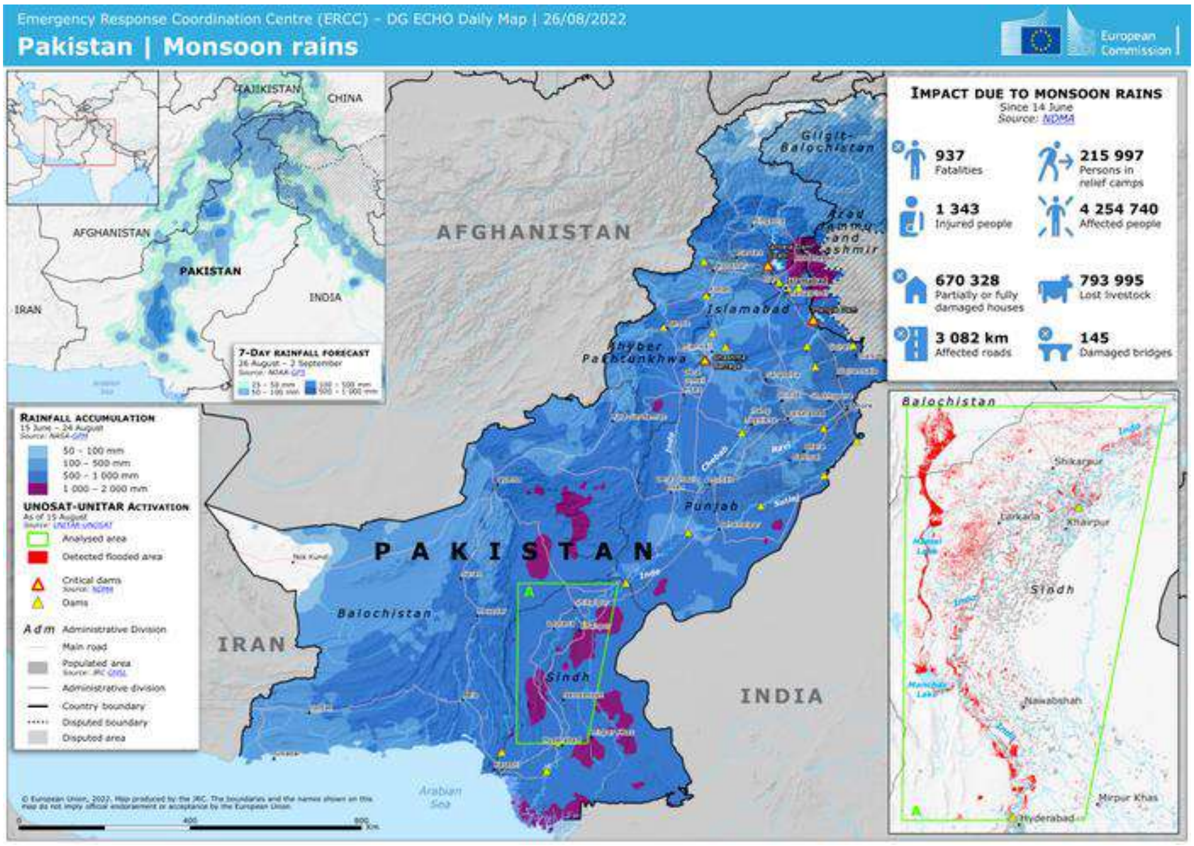

Pakistan Monsoon rains - DG ECHO Daily Map | 26/08/2022 - Pakistan | ReliefWeb (Source NDMA)

Annex B Topographic Survey

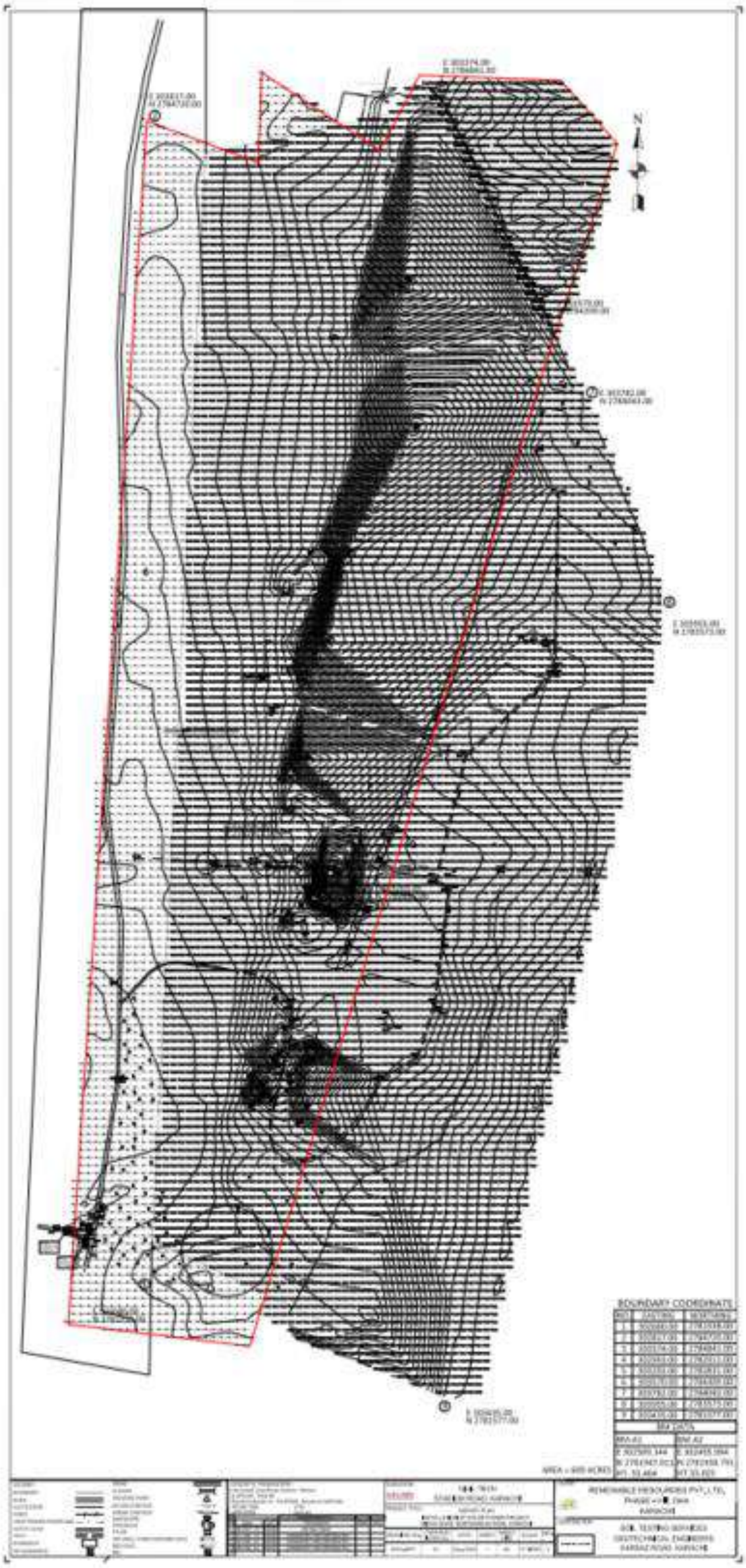

Annex C HEC-RAS Model Computations

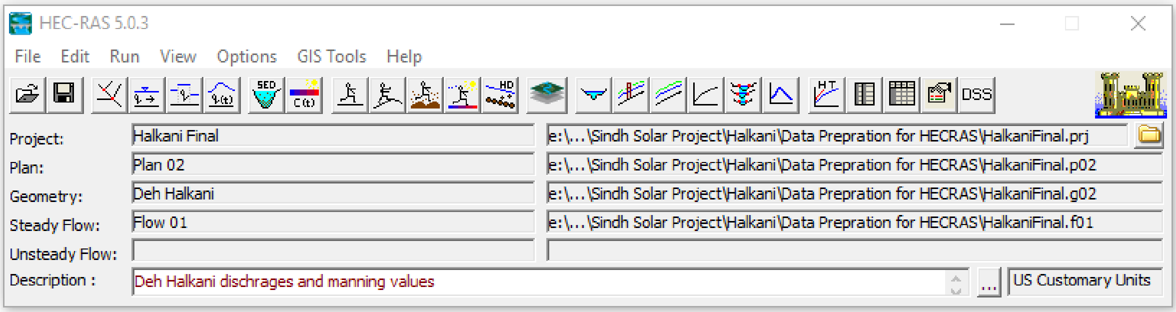

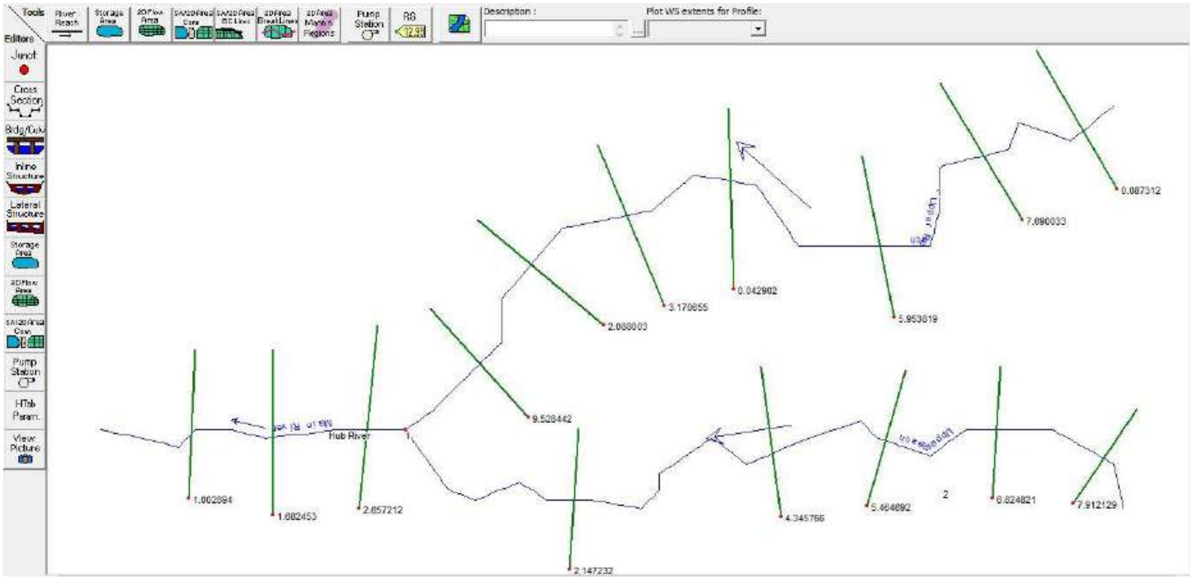

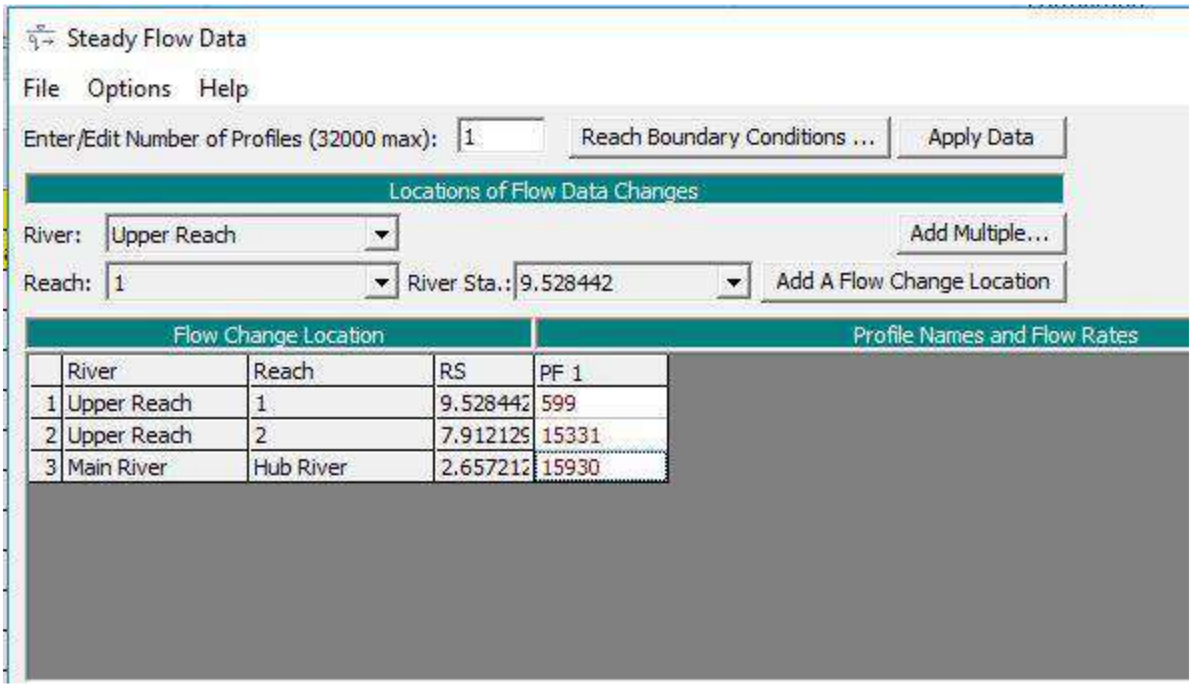

	River	Reach	RS	PF 1
1	Upper Reach	1	9.528442	599
2	Upper Reach	2	7.912129	15331
3	Main River	Hub River	2.657212	15930

Annex D Temperature data (1999-2022) [7]

Halkani													
Years	Jan	Feb	March	Apr	May	Jun	Jul	Aug	Sept	Oct	Nov	Dec	G Annum Temp °C
1999	18.96	22.01	24.58	28.77	30.12	30.41	29.29	28.31	28.05	28.87	25.19	20.37	26.26
2000	19.25	20.61	24.97	29.00	30.17	30.32	29.49	28.47	28.05	27.96	24.96	21.17	26.21
2001	19.18	22.25	25.44	27.91	30.10	30.25	29.02	28.48	28.56	28.66	25.62	22.79	26.54
2002	19.71	21.05	25.89	28.64	30.32	30.67	28.96	28.07	26.86	28.79	25.20	21.30	26.31
2003	20.21	22.20	25.25	29.56	29.66	30.25	29.59	28.81	27.99	28.47	23.94	20.43	26.38
2004	19.45	22.30	27.08	29.23	30.42	30.65	29.21	28.34	27.92	27.58	25.40	21.69	26.61
2005	18.77	20.73	25.10	28.17	29.84	31.08	29.37	28.27	29.18	28.34	25.37	20.19	26.22
2006	18.57	23.97	25.09	27.99	29.66	30.18	29.51	27.93	29.30	29.06	26.13	19.88	26.44
2007	19.91	22.59	24.48	28.84	30.31	31.26	30.59	29.08	29.53	28.00	25.51	19.63	26.65
2008	17.67	19.39	25.99	28.14	29.43	30.94	29.44	28.50	28.91	28.58	24.57	20.35	26.01
2009	20.15	22.81	25.98	28.77	30.95	30.98	29.98	29.18	28.69	28.27	24.65	21.15	26.81
2010	20.04	21.38	26.71	29.04	30.77	30.10	30.19	29.18	28.92	28.51	25.43	19.79	26.70
2011	19.02	21.60	25.43	28.27	29.91	30.52	29.70	29.09	28.54	27.79	26.24	20.66	26.42
2012	18.70	19.78	24.54	28.40	30.14	29.98	29.37	28.61	29.34	28.39	25.74	21.03	26.18
2013	19.42	21.47	25.73	27.98	30.15	31.50	29.78	28.40	28.75	29.45	25.23	20.61	26.56
2014	17.98	20.76	24.69	28.13	30.21	31.49	29.99	29.21	28.90	28.65	25.65	20.46	26.37
2015	19.30	22.20	24.84	29.24	30.63	32.17	29.88	28.78	29.44	29.23	25.54	20.40	26.82
2016	20.99	22.37	25.99	28.08	30.30	30.86	30.12	29.21	28.41	27.80	24.80	22.50	26.80
2017	18.63	22.09	25.21	28.81	30.54	31.35	29.60	29.01	28.41	28.96	24.59	20.02	26.45
2018	20.46	22.61	26.31	29.15	31.56	30.95	30.03	28.36	27.66	28.73	26.09	20.54	26.89
2019	19.38	20.59	24.36	28.42	30.06	31.90	30.65	29.14	30.14	29.01	24.84	19.64	26.53
2020	17.45	22.17	24.34	28.68	30.48	31.74	31.94	30.44	30.04	29.02	23.45	19.62	26.62
2021	17.91	22.91	26.48	29.51	31.26	31.14	30.39	28.68	30.66	27.84	25.09	20.00	26.83
2022	18.03	22.31	26.66	29.34	30.23	30.32	29.34	28.75	28.86	28.05	24.94		27.01
GM Avg	**19.13**	**21.75**	**25.46**	**28.67**	**30.30**	**30.88**	**29.81**	**28.76**	**28.80**	**28.50**	**25.17**	**20.62**	**26.52**

[7] https://www.ncei.noaa.gov/access/past-weather/26.68796005351616,65.31836031280113,24.117410176472962,70.53608327857864

Annex E Annual Rainfall (mm) [8]

Years	Jan	Feb	March	Apr	May	Jun	Jul	Aug	Sept	Oct	Nov	Dec	G Annum ppt (mm)
1999	6.5	0.4	9.5	0	6.7	3.7	8.9	1.3	2.6	19.2	0	0	58.8
2000	3.4	1.5	0	0	2.7	5.5	6.2	34.8	1.6	0	0	0.7	56.4
2001	0	0	0.1	0.1	3.5	6	43	57.6	3.2	2	0	0.1	115.6
2002	0	0.8	0	0	1.1	1.2	19	18.9	4.4	0	1.1	1.1	47.6
2003	3.5	3	0	0	0.7	5.3	219.8	6.6	1.6	0	0.2	0	240.7
2004	9	0	0	0.1	0.3	10.9	16.1	10.3	5.5	11	0	3.2	66.4
2005	7.8	12.7	1.6	0.1	0.6	4.7	9.7	12.8	11.3	0	0	0	61.3
2006	0	0	2.2	0	0.5	5.6	81.1	110	0.7	2.3	0	20.4	222.8
2007	0	19.5	24.9	0	0.6	93.5	17	59.3	3.7	0	0	13.7	232.2
2008	9.3	4.4	0.1	2.8	0.2	2.6	16.6	23.5	0.4	0	0	34.1	94
2009	2.7	0.4	0.1	0	0.5	1.9	88.8	20.3	17	0	0	0.7	132.4
2010	0.1	9.5	0	0	0	48.5	107.6	48.8	30.6	1.7	0	0	246.8
2011	0.2	6.1	0.3	1.1	0	6.9	43.7	74	118.6	2.1	12.4	0	265.4
2012	4.1	0	0.1	1.5	0	1.7	9	13.3	37.1	1	0	2.2	70
2013	1.3	3.2	1.6	5.9	0.8	8.7	27.9	75.2	8.8	5.9	0	0	139.3
2014	0	0.7	5	3.4	2.2	4.5	34.5	10.8	2.9	5.8	4	0	73.8
2015	1.2	2.7	2.7	1.2	1.6	6.7	42.8	6.8	0.4	0.2	0	0	66.3
2016	1.7	0	4.8	0	0.4	15.9	15.3	65	2.1	0	0	0.6	105.8
2017	12.6	0.6	0.1	0	0	24.1	66	64.7	4.9	0	0	7.7	180.7
2018	0	0.2	0	1.4	0	12.5	5.2	14.4	3.2	0	0	0.3	37.2
2019	14.2	3.6	4.7	1.1	0.1	2.1	67.6	173.3	49.9	11.8	3.6	0.3	332.3
2020	6	0.2	3.1	0	1	2.4	23.5	109.6	8.8	0	6.8	0	161.4
2021	0	0	0	0.2	0.1	3.8	39.7	6.1	49.3	21.6	0	12.8	133.6
2022	23.3	0.3	0	0	0.1	11.4	295.5	182.4	6.3	0	2.1	2.3	521.4
GM Sum	**106.9**	**69.8**	**60.9**	**18.9**	**23.7**	**290.1**	**1304.5**	**1199.8**	**374.9**	**84.6**	**30.2**	**97.9**	**3662.2**

[8] https://www.ncei.noaa.gov/access/past-weather/26.68796005351616,65.31836031280113,24.117410176472962,70.53608327857864

Annex F Project Site Pictures